12 The Neutrinos

"The neutrino is the smallest bit of material reality ever conceived of by man; the largest is the universe. To attempt to understand something of one in terms of the other is to attempt to span the dimension in which lie all manifestations of natural law." These comments were made in 1956 by Cowan and Reines in their report on the definite evidence of the neutrino[1], the elementary particle that Pauli postulated 26 years earlier in his attempt to explain the continuous energy spectrum of the electrons emitted by β-decays of nuclei: $\mathcal{N}_1(Z) \to \mathcal{N}_2(Z+1) + \mathrm{e}^- + \overline{\nu}_\mathrm{e}$.

Many years later, the acute insight of the neutrino discoverers remains astonishingly topical. Because of their abundance in nature, if the neutrinos have a tiny but nonzero mass, they would play a crucial role in the evolution of the universe and fulfill their mission of bridging the gap separating the two extreme scales of physics. So the first three sections are devoted to the question of their masses, through the fascinating possibility for neutrino species to transmute into each other (a process called neutrino oscillations) and a related problem known as the solar ν_e deficit. Next, the crucial role of neutrinos in the discovery of weak neutral currents is emphasized, in relation to the neutrino scattering by the electron. The evidence for neutral currents in turn leads to the confirmation of the standard model and the prediction of the gauge boson $\mathrm{W}^\pm$ and Z^0 masses, long before their observations. Finally, deep inelastic neutrino–nucleon collision is shown to be a powerful probe of the quark and gluon constituents of matter. Neutrinos and electrons play complementary roles in their respective weak and electromagnetic reactions which may be exploited to determine the quark fractional charges. All of these topics constitute the core of the standard electroweak theory and its possible extensions for which an active research on the neutrino masses is crucial.

12.1 On the Neutrino Masses

Three neutrino species are known to exist: the electron neutrino ν_e, the neutrino ν_μ associated with the muon and the neutrino ν_τ associated with

[1] *Nature* **178** (1956) 446. In fact, it was the antineutrino $\overline{\nu}_\mathrm{e}$ emitted in nuclei β-decay (Savannah River reactor).

the τ lepton. Until now evidence for the existence of ν_τ is only indirect from the τ decay modes, in contrast with the first two ν_e and ν_μ which are directly observed. Altogether, there are now six leptons in nature: three neutral (ν_e , ν_μ , ν_τ) and three charged (e^- , μ^- , τ^-), as well as the six corresponding antileptons. One of the most remarkable experiments performed on the LEP collider at CERN is the establishment of the number of neutrino species that have exactly the *same properties* as the ν_e (identical V − A coupling, massless or almost massless). There must exist only three neutrino families, otherwise the Z^0 width would exceed its current value by at least 167 MeV (see Problem 9.5).

In distinction with all other fermions, the neutrinos are sensible only to weak interactions. The following example may illustrate the distinctive character of these unique particles: of the sixty billions or so of neutrinos that come out of the sun and that pass through each cm^2 of the earth surface per second, very few will interact with matter, the cross-section of neutrino interacting with matter being so vanishingly small.

12.1.1 General Properties

In the Glashow–Salam–Weinberg (GSW) standard model, the following assumptions on the neutrinos are explicitly made:

(i) their masses are identically zero;

(ii) only their left-handed components $\psi_L \equiv \frac{1}{2}\big(1-\gamma_5\big)\psi$ are operative in physical processes.

The right-handed components of neutrinos $\psi_R \equiv \frac{1}{2}\big(1+\gamma_5\big)\psi$, even if they exist, do not interact with other particles and are thus absent from the Lagrangian. We also recall that for a massless fermion, $\boldsymbol{\sigma}\cdot\widehat{\boldsymbol{p}}\,\psi_L = -\psi_L$, i.e. the left-handed neutrino is also the eigenstate of the helicity operator $\boldsymbol{\sigma}\cdot\widehat{\boldsymbol{p}}$ with eigenvalue -1, its spin $\boldsymbol{\sigma}$ is antiparallel to its three-momentum $\boldsymbol{p}$. If the neutrino is left-handed, the antineutrino is right-handed (its spin is then parallel to its momentum). These properties are explicit in the Weyl representation, suitable for two-component massless neutrinos (Chap. 3).

The second assumption (ii) is based on, among others, the experimental observation of the electron asymmetry from a polarized nucleus in its β-decay (Sect. 5.1), on the energy and asymmetry distributions of the electron in μ and τ decays (Chap. 13), and on the direct determination of the neutrino helicity in a key experiment by Goldhaber et al. (Further Reading). All of these data definitely establish the V − A character of the charged currents.

Because of these assumptions, there is a distinction between the leptons and the quarks in their weak interactions with the gauge bosons $W^\pm$, Z^0. To describe these interactions (see Table 9.5), the left-handed fermions are put in SU(2) doublets and the right-handed fermions in U(1) singlets. Only left-handed doublets are coupled to $W^\pm$, while both left and right components couple to Z^0. In the leptonic sector, we remark the absence of right-handed neutrinos ν_R and of mixing between the lepton families, to be contrasted with the Cabibbo–Kobayashi–Maskawa (CKM) mixing among the quark families.

12.1.2 Dirac or Majorana Neutrino?

A neutral fermion may exist either as a Dirac particle (fermion $\neq$ antifermion) or as a Majorana particle (fermion $\equiv$ antifermion). For a Dirac fermion (neutral or charged), the mass term is $-m\,\overline{\psi}\psi = -m\,(\overline{\psi}_{\rm R} + \overline{\psi}_{\rm L})(\psi_{\rm R} + \psi_{\rm L}) = -m\,(\overline{\psi}_{\rm R}\psi_{\rm L} + \overline{\psi}_{\rm L}\psi_{\rm R})$ since $\overline{\psi}_{\rm R}\psi_{\rm R}$ and $\overline{\psi}_{\rm L}\psi_{\rm L}$ vanish using (9.7)–(9.9). The mass term always connects the opposite chiral components of the same field. The absence of either, $\psi_{\rm R}$ or $\psi_{\rm L}$, automatically leads to $m = 0$.

If the neutrinos are of the Majorana type, even in the absence of right-handed components, we can build a mass term by using the antiparticle which is identical to its conjugate, only with opposite chirality. Indeed, contrary to charged fermions, the neutrino and the antineutrino, being chargeless, can be self-conjugated $\nu_{\rm M} \equiv \nu_{\rm M}^c$. They are called the Majorana neutrino $\nu_{\rm M}$.

To each fermionic field ψ there corresponds the field of its antiparticle, denoted by ψ^c, obtained with the help of the charge conjugation operator $\mathcal{C} = {\rm i}\gamma^2\gamma^0$ (Chap. 5). We have $\psi^c \equiv \mathcal{C}\psi\mathcal{C}^{-1} = {\rm i}\gamma^2\gamma^0\overline{\psi}^T = {\rm i}\gamma^2\psi^*$. The field of a fermion F is ψ and the field of its antifermion $\overline{F}$ is ψ^c.

While for a charged fermion $m\overline{\psi}\psi$ is the only possible mass term, for a neutral fermion there are other possibilities. In addition to the standard term $\overline{\psi}\psi$, the terms $\overline{\psi^c}\psi^c$, $\overline{\psi}^c\psi$, and $\overline{\psi}\psi^c$ are equally valid. The first $\overline{\psi}^c\psi^c$ is equivalent to $\overline{\psi}\psi$, but the last two, $\overline{\psi}^c\psi$ and $\overline{\psi}\psi^c$, may be written respectively as $\overline{\psi}^c_{\rm L}\psi_{\rm L} + \overline{\psi}^c_{\rm R}\psi_{\rm R}$ and $\overline{\psi}_{\rm L}\psi^c_{\rm L} + \overline{\psi}_{\rm R}\psi^c_{\rm R}$. Indeed

$$\psi^c_{\rm L} \equiv (\psi_{\rm L})^c = \mathcal{C}\psi_{\rm L}\mathcal{C}^{-1} = {\rm i}\gamma^2\psi^*_{\rm L} = \tfrac{1}{2}\,(1+\gamma_5)\psi^c\ ,$$

$$\psi^c_{\rm R} \equiv (\psi_{\rm R})^c = \mathcal{C}\psi_{\rm R}\mathcal{C}^{-1} = {\rm i}\gamma^2\psi^*_{\rm R} = \tfrac{1}{2}\,(1-\gamma_5)\psi^c\ ,$$

$$\overline{\psi}^c_{\rm L} = \overline{\psi}^c\,\tfrac{1}{2}\,(1-\gamma_5), \qquad \overline{\psi}^c_{\rm R} = \overline{\psi}^c\,\tfrac{1}{2}\,(1+\gamma_5)\ .$$

If the neutrino is a Majorana fermion, we can always construct a mass term $\overline{\psi}^c_{\rm L}\psi_{\rm L} + \overline{\psi}_{\rm L}\psi^c_{\rm L}$ without the right-handed component $\psi_{\rm R}$ *precisely because* $\psi^c_{\rm L}$ *is right-handed with positive helicity.*

The existence of Majorana neutrinos implies that their interactions violate the leptonic number L_ℓ. Since $\nu_{\rm M}$ is $(\psi + \psi^c)/\sqrt{2}$, the weak charged current connecting the electron to the Majorana neutrino contains both $L_{\rm e} = \pm 1$ terms. The most spectacular manifestation of $\nu_{\rm M}$ would be the neutrinoless double β-decay of nuclei $\mathcal{N}_1(Z) \to \mathcal{N}_2(Z+2) + {\rm e}^- + {\rm e}^-$ (Fig. 12.1a), denoted by $(\beta\beta)_{0\nu}$. The initial state has zero leptonic quantum number ($L_{\rm e} = 0$), while the final state with two electrons has $L_{\rm e} = 2$. In $(\beta\beta)_{0\nu}$, the Majorana neutrino $\nu_{\rm M}$ emitted by ${\rm n} \to {\rm p} + {\rm e}^- + \nu_{\rm M}$ can be absorbed by the second neutron ${\rm n}'$ to become ${\rm p}' + {\rm e}^-$. This is because $\nu_{\rm M}$ does not have a well-defined lepton number; when emitted by n , it has $L_{\rm e} = -1$ and when reabsorbed by ${\rm n}'$, it has $L_{\rm e} = +1$.

On the other hand, with the Dirac neutrino for which the leptonic number is conserved, double β-decay $\mathcal{N}_1(Z) \to \mathcal{N}_2(Z+2) + {\rm e}^- + {\rm e}^- + \overline{\nu}_{\rm e} + \overline{\nu}_{\rm e}$ (Fig. 12.1b), referred to as $(\beta\beta)_{2\nu}$, can only occur with two antineutrinos $\overline{\nu}_{\rm e}$

emitted together with two electrons. Unlike the $\nu_{\rm M}$, the Dirac $\overline{\nu}_{\rm e}$ emitted in $\mathrm{n} \to \mathrm{p} + \mathrm{e}^- + \overline{\nu}_{\rm e}$ cannot be absorbed by n' to become $\mathrm{p}' + \mathrm{e}^-$.

By energy-momentum conservation, the energy spectrum of the two-electron system in $(\beta\beta)_{2\nu}$ decay with Dirac neutrinos is continuous. In $(\beta\beta)_{0\nu}$ by Majorana neutrinos, the same two-electron energy spectrum has a sharp peak (ideally a delta function) which is the distinctive signature of this decay mode. The amplitudes of both $(\beta\beta)_{2\nu}$ and $(\beta\beta)_{0\nu}$ are of the second order in the Fermi constant $G_{\rm F}$, therefore their rates are very low; nevertheless positive results of the standard decay mode $(\beta\beta)_{2\nu}$ have been reported[2] for nine different isotopes, with half-lives in the range of $10^{19} - 10^{24}$ years. Experiments have been carried out to observe neutrinoless $(\beta\beta)_{0\nu}$ decays of the ^{136}Xe, ^{76}Ge , ^{48}Ca isotopes, but the results were not conclusive[2]. If the electron–$\nu_{\rm M}$ mixing ($V_{\rm lep}$ below) is small, and/or if the $\nu_{\rm M}$ mass is too small (through the $\nu_{\rm M}$ propagator effect), then $(\beta\beta)_{0\nu}$ may still escape observation.

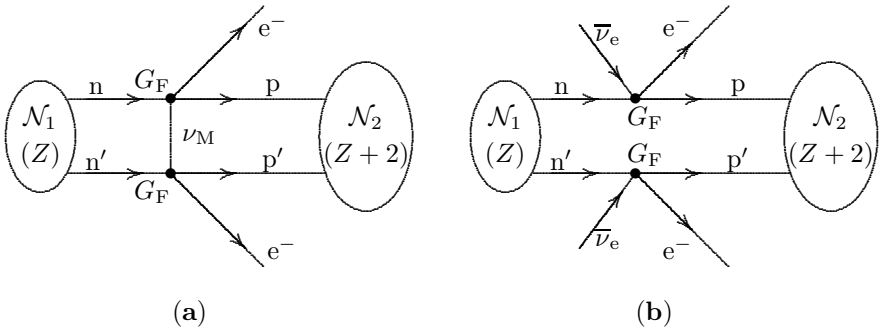

Fig. 12.1. (**a**) Double neutrinoless $(\beta\beta)_{0\nu}$ decay by Majorana neutrino; (**b**) double $(\beta\beta)_{2\nu}$ decay by Dirac neutrino

Remarks. (i) Unlike the electromagnetic U(1) *local* symmetry, the leptonic number symmetry does not govern the dynamics; rather it is a consequence of the dynamics and the field contents of the standard model. In other words, there is nothing sacred about the leptonic number conservation. If this quantum number is broken, the left-handed neutrino $\nu_{\rm L}$ and the right-handed antineutrino $\nu_{\rm R}^{\rm c}$ will constitute the left- and right-handed components of the same field (the Majorana neutrino) and a mass term with only $\nu_{\rm L}$ can be constructed. This self-conjugacy is the reason why a Majorana field can be described only by two-component complex spinors, while the Dirac field needs four-component complex spinors. The former has only half as many degrees of freedom as the latter. The situation is analogous to the neutral π and K mesons: the π^0, which is its own antiparticle, can be represented by a real scalar field, while it is necessary to have a complex scalar field to distinguish K^0 from $\overline{\mathrm{K}}^0$.

[2] M.K.Moe, *Neutrino* 94, Nucl. Phys. (Proc. Suppl.) **B38** (1995)

(ii) For different reasons, both the Majorana and the Weyl fields are two-component spinors. For the Majorana particle, because it is self-conjugate; for the Weyl particle, which is distinct from its antiparticle, because it is massless.

12.1.3 Lepton Mixing

In any case, whether of the Dirac type or of the Majorana type, massless neutrinos of different families do not mix up, contrary to quarks. If the neutrinos are massless, i.e. degenerate in mass, the leptonic flavors are not mixed. All states with degenerate masses are physically equivalent and are the eigenstates of their common mass operator. This implies the absence of nondiagonal charged currents like $\overline{\nu}_{\mathrm{e}}\gamma_\lambda(1-\gamma_5)\mu$ (symbolically written as $\overline{\nu}_{\mathrm{e}}\mu$). The six nondiagonal charged currents $\overline{\nu}_{\mathrm{e}}\mu$, $\overline{\nu}_{\mathrm{e}}\tau$, $\overline{\nu}_{\mu}\mathrm{e}$, $\overline{\nu}_{\mu}\tau$, $\overline{\nu}_{\tau}\mathrm{e}$, and $\overline{\nu}_{\tau}\mu$ do not exist, there remain only three diagonal currents $\overline{\nu}_{\mathrm{e}}\mathrm{e}$, $\overline{\nu}_{\mu}\mu$, and $\overline{\nu}_{\tau}\tau$ that separately conserve their respective leptonic numbers $L_{\mathrm{e}}, L_\mu, L_\tau$. Consequently, all leptonic flavor-changing reactions like $\nu_\mu + \mathrm{n} \to \mathrm{e}^- + \mathrm{p}$, $\mu^\pm \to \mathrm{e}^\pm + \gamma$, etc. (Problem 12.1) are forbidden, whereas hadronic flavor-changing reactions, like $\mathrm{D} \to \overline{\mathrm{K}} + \mathrm{e}^+ + \nu_{\mathrm{e}}$, $\mathrm{B} \to \overline{\mathrm{D}}^* + \rho$, and $\mathrm{K}^\pm \to \pi^\pm + \pi^0 + \gamma$ coming respectively from $\mathrm{c} \to \mathrm{s}$, $\overline{\mathrm{b}} \to \overline{\mathrm{c}}$, and $\mathrm{s} \to (\mathrm{u},\mathrm{c}) \to \mathrm{d}$ are allowed and observed. The latter mode, although rare because of higher-order effects (penguin diagrams, as in Chap. 11), nevertheless exists.

In the standard model, neutrinos are assumed massless simply because a firm proof of nonzero lower bounds of their masses is still lacking, the averages of terrestrial (noncosmic) direct measurements give only their upper bounds $m(\nu_{\mathrm{e}}) < 15\,\mathrm{eV}$, $m(\nu_\mu) < 170\,\mathrm{KeV}$, $m(\nu_\tau) < 19.3\,\mathrm{MeV}$.

Nevertheless, the two hypotheses of the GSW standard model mentioned above demand close scrutiny for many reasons: first, the neutrino helicity is measured with large errors (at 10% of accuracy at best); second, it seems impossible to demonstrate experimentally that the neutrino mass is identically zero. Moreover, the masslessness of fermions has no deep theoretical foundation, in contrast to the massless photon demanded by local gauge invariance. If the neutrinos turn out to be massive, then like the three quark families, the three lepton families could get mixed up, and the presumably small neutrino masses could be indirectly revealed by the oscillation phenomenon analogous to the neutral K-meson oscillations considered in the previous chapter. The mixing of massive neutrinos may follow one of two different scenarios. The first, identical to that for quarks, involves Dirac neutrinos which acquire masses through the usual Higgs mechanism. The second involves Majorana neutrinos whose masses are generated only in models beyond the standard model.

The existence and the size of the neutrino masses are of essential importance in particle physics and astrophysics. In particular, given the enormous abundance of the neutrinos in the universe, solutions to the problems of dark matter, the missing mass, and the expansion rate of the universe will depend crucially on whether the neutrinos are massive or not.

Through their oscillations, massive neutrinos could explain the solar neutrino deficit observed continuously for the last thirty years in the Homestake mines (USA) and actively investigated in different underground experiments: GALLEX (Italy), Kamiokande (Japan), SNO (Canada), and SAGE (Russia). The solar neutrino deficit may be briefly described as follows. The ν_{e} flux – produced inside the sun by thermonuclear reactions and measured in these experiments – is lower than predicted by sophisticated calculations within the standard solar model. The ν_{e} loss, if it is true, could be attributed to its conversion into ν_μ (and/or ν_τ) through oscillations due to their nonzero masses.

12.2 Oscillations in the Vacuum

The quantum oscillation phenomenon occurs when a particle produced by a reaction is not identically the same as the particle that subsequently propagates and decays. The best-known example is the neutral K mesons considered previously. The system $\mathrm{K}^0, \overline{\mathrm{K}}^0$ produced by strong interactions are distinct from the set $\mathrm{K_L}$, $\mathrm{K_S}$ which are governed by weak interactions. The K^0 and $\overline{\mathrm{K}}^0$ are distinguished by their associated production (Chap. 11); whereas the $\mathrm{K_L}$, $\mathrm{K_S}$, each with a distinctive mass, are characterized by their decay modes. In this context, let us call the former the eigenstates of the strong interaction and the latter, the eigenstates of the weak interaction. The neutral K system oscillates, as we know, since there exists a transition connecting the strong interaction eigenstates $\mathrm{K}^0, \overline{\mathrm{K}}^0$ to the weak eigenstates $\mathrm{K_L}$, $\mathrm{K_S}$.

Following the example of $\mathrm{K_L}$ and $\mathrm{K_S}$ defined as a combination of K^0 and $\overline{\mathrm{K}}^0$ through (11.3), let us introduce two mass eigenstates ν_1 and ν_2 (of masses m_1 and m_2) such that we can imagine the physical weakly interacting eigenstates ν_{e} and ν_μ as linear combinations of ν_1 and ν_2:

$$\begin{pmatrix} \nu_{\mathrm{e}} \\ \nu_\mu \end{pmatrix} \equiv U(\theta) \begin{pmatrix} \nu_1 \\ \nu_2 \end{pmatrix} \equiv \begin{pmatrix} \cos\theta & \sin\theta \\ -\sin\theta & \cos\theta \end{pmatrix} \begin{pmatrix} \nu_1 \\ \nu_2 \end{pmatrix} . \tag{12.1}$$

We can pursue the analogy with the quark sector. We recall that the three left-handed quark doublets in Table 9.5 [thoses defined by (9.176) and (9.177)] can also be written as:

$$\begin{pmatrix} \mathrm{u}'' \\ \mathrm{d} \end{pmatrix}_{\mathrm{L}} , \quad \begin{pmatrix} \mathrm{c}'' \\ \mathrm{s} \end{pmatrix}_{\mathrm{L}} , \quad \begin{pmatrix} \mathrm{t}'' \\ \mathrm{b} \end{pmatrix}_{\mathrm{L}} , \text{ where } \begin{pmatrix} \mathrm{u}'' \\ \mathrm{c}'' \\ \mathrm{t}'' \end{pmatrix} = \begin{pmatrix} V_{\mathrm{ud}} & V_{\mathrm{us}} & V_{\mathrm{ub}} \\ V_{\mathrm{cd}} & V_{\mathrm{cs}} & V_{\mathrm{cb}} \\ V_{\mathrm{td}} & V_{\mathrm{ts}} & V_{\mathrm{tb}} \end{pmatrix}^{\dagger} \begin{pmatrix} \mathrm{u} \\ \mathrm{c} \\ \mathrm{t} \end{pmatrix}$$

In the same way that the weak interaction eigenstates $\mathrm{u}'', \mathrm{c}'', \mathrm{t}''$ are linear combinations of the mass eigenstates u, c, t of masses m_{u}, m_{c}, m_{t} via the $V_{\mathrm{CKM}}^{\dagger}$ mixing matrix, the weakly interacting neutrino eigenstates ν_{e}, ν_μ, ν_τ – analogous to $\mathrm{u}'', \mathrm{c}'', \mathrm{t}''$ – are linear combinations of ν_1, ν_2, ν_3, the neutrino mass eigenstates of masses m_1, m_2, m_3.

The lepton mixing is realized by a 3×3 unitary matrix $\mathrm{V_{lep}}$:

$$\begin{pmatrix} \nu_{\mathrm{e}} \\ \mathrm{e}^- \end{pmatrix}_{\mathrm{L}} , \quad \begin{pmatrix} \nu_\mu \\ \mu^- \end{pmatrix}_{\mathrm{L}} , \quad \begin{pmatrix} \nu_\tau \\ \tau^- \end{pmatrix}_{\mathrm{L}} \quad \text{where} \quad \begin{pmatrix} \nu_{\mathrm{e}} \\ \nu_\mu \\ \nu_\tau \end{pmatrix} = \mathrm{V_{lep}} \begin{pmatrix} \nu_1 \\ \nu_2 \\ \nu_3 \end{pmatrix}$$

The idea of neutrino oscillations was put forth for the first time by Pontecorvo, and the mixing (1) was suggested by Maki, Nakagawa, and Sakata even before its analog in the hadronic sector was proposed by Cabibbo. Like the V_{CKM} quark-mixing matrix, the $\mathrm{V_{lep}}$ can only be determined by experiment. In the present state of our knowledge, the standard model does not pretend to predict either the masses of the fermions or their mixings. The determination of these parameters is one of the most fascinating problems and is actively investigated in particle physics. Observations of neutrino oscillations seem to be the best (maybe unique) method to measure their eventual nonzero tiny masses and $\mathrm{V_{lep}}$. To illustrate the phenomenon, let us only consider the two families ν_{e} and ν_μ using the submatrix $U(\theta)$ of $\mathrm{V_{lep}}$. This simplification avoids complications of a 3×3 matrix without losing any physical understanding.

First, we show that when the muon-neutrino ν_μ propagates, it oscillates between ν_μ and ν_{e} because of the mass difference, $m_1 \neq m_2$. Then ν_μ is partially converted into ν_{e}, just as K^0 becomes partially $\overline{\mathrm{K}}^0$. Indeed, the evolution of the mass eigenstates $\nu_1(t), \nu_2(t)$ at the time $t > 0$ is given by

$$\nu_1(t) = \nu_1(0)\mathrm{e}^{-\mathrm{i}E_1 t} \quad , \quad \nu_2(t) = \nu_2(0)\mathrm{e}^{-\mathrm{i}E_2 t} \, , \tag{12.2}$$

where $E_j^2 = |\boldsymbol{p}_j|^2 + m_j^2$. For relativistic neutrinos, which is always the case since $m_j \ll |\boldsymbol{p}_j|$, we have $|\boldsymbol{p}_1| = |\boldsymbol{p}_2| = |\boldsymbol{p}| \approx E$ and $E_j \approx E + m_j^2/2E$. Putting (2) into (1) we get

$$\begin{aligned} \nu_\mu(t) &= [\mathrm{e}^{-\mathrm{i}E_1 t} \sin^2\theta + \mathrm{e}^{-\mathrm{i}E_2 t} \cos^2\theta]\nu_\mu(0) + \cos\theta \sin\theta [\mathrm{e}^{-\mathrm{i}E_2 t} - \mathrm{e}^{-\mathrm{i}E_1 t}]\nu_{\mathrm{e}}(0) \, , \\ \nu_{\mathrm{e}}(t) &= [\mathrm{e}^{-\mathrm{i}E_1 t} \cos^2\theta + \mathrm{e}^{-\mathrm{i}E_2 t} \sin^2\theta]\nu_{\mathrm{e}}(0) + \cos\theta \sin\theta [\mathrm{e}^{-\mathrm{i}E_2 t} - \mathrm{e}^{-\mathrm{i}E_1 t}]\nu_\mu(0) \, . \end{aligned} \tag{12.3}$$

The probability for a muon-neutrino ν_μ produced at $t = 0$ remains the same particle ν_μ at $t > 0$ is then given by

$$\begin{aligned} P(\nu_\mu \to \nu_\mu, t) &\equiv |\, \langle \nu_\mu(t) \,|\nu_\mu(0)\rangle \,|^2 \\ &= 1 - \frac{1}{2}\sin^2 2\theta + \frac{1}{2}\sin^2 2\theta \;\; \cos\left(\frac{\triangle m_{21}^2}{2E}\, t\right) \\ &= 1 - \sin^2 2\theta \;\; \sin^2\left(\frac{\triangle m_{21}^2}{4E}\, t\right) = P(\nu_{\mathrm{e}} \to \nu_{\mathrm{e}}, t) \, , \end{aligned} \tag{12.4}$$

where $\triangle m_{21}^2 \equiv m_2^2 - m_1^2$. The probability for ν_μ to be converted into ν_{e} at $t > 0$ is then

$$P(\nu_\mu \to \nu_{\mathrm{e}}, t) = \sin^2 2\theta \;\; \sin^2\left(\frac{\triangle m_{21}^2}{4E}\, t\right) = P(\nu_{\mathrm{e}} \to \nu_\mu, t) \, . \tag{12.5}$$

Because of their presumed tiny masses, neutrinos are ultra-relativistic. The distance they travel from their production source to a detector is $L = t$ ($c = 1$ in natural units), such that if L is much larger than $2E/|\triangle m^2_{21}|$, the rapidly fluctuating cosine term in (4) vanishes on the average, and the transitions $\nu_\mu \to \nu_\mu, \nu_\mu \to \nu_\mathrm{e}$ become constant in space L and time t. The oscillations average to zero.

The conditions for oscillations to appear are: both θ and $\triangle m^2_{21}$ have nonzero values, and the traveling distance L of the neutrino must not differ too much from the oscillation length L_osc defined by

$$L_\mathrm{osc} \equiv \frac{4\pi E}{|\triangle m^2_{21}|} = 2.48 \times \frac{E/(\mathrm{MeV})}{|\triangle m^2_{21}|/(\mathrm{eV})^2}\ \mathrm{m}\ . \tag{12.6}$$

If $L \gg L_\mathrm{osc}$, $\cos(\triangle m^2_{21} t/2E) = \cos(2\pi L/L_\mathrm{osc})$ is zero on the average and oscillations cannot be observed. In this case, the sine term in (4) and (5) i.e. $\sin^2\left(\triangle m^2_{21} t/4E\right) = \sin^2(\pi L/L_\mathrm{osc})$ can be effectively replaced with $1/2$.

When $\triangle m^2_{21}$ is expressed in $(\mathrm{eV})^2$, E in MeV, and L in meters, (4) and (5) are written numerically as

$$\begin{aligned} P(\nu_\mu \to \nu_\mu, t) &= 1 - \sin^2 2\theta\ \ \sin^2\left(\frac{1.27\triangle m^2_{21} L}{E}\right)\ , \\ P(\nu_\mu \to \nu_\mathrm{e}, t) &= \sin^2 2\theta\ \ \sin^2\left(\frac{1.27\triangle m^2_{21} L}{E}\right)\ . \end{aligned} \tag{12.7}$$

These equations tell us that oscillations could be observed in many different experiments, provided that $|\triangle m^2_{21}|$ belongs to the ranges given in Table 12.1. In turn this Table shows that explorations of several neutrino sources are necessary to cover the completely unknown domain of $|\triangle m^2_{21}|$.

Table 12.1. Typical ranges of parameters in neutrino oscillations

Source	Energy E (MeV)	Distance L (m)	$\lvert\triangle m^2_{21}\rvert$ $(\mathrm{eV})^2$
Reactor	$1 - 10$	$10 - 100$	$1 - 10^{-2}$
Accelerator	$10^3 - 10^5$	$10^2 - 10^3$	$10^3 - 1$
Atmosphere	$10^2 - 10^3$	$10^4 - 10^7$	$10^{-1} - 10^{-5}$
Solar core	$10^{-1} - 10$	10^{11}	$10^{-10} - 10^{-12}$

The neutrino transmutations are usually plotted in the plane $x = \sin^2 2\theta$, $y = |\triangle m^2_{21}|$ (in units of eV^2) where the allowed (forbidden) regions are exhibited. The data are illustrated in Fig. 12.2 in which the point ($x = 0$, $y = 0$) is not definitely excluded for the time being. The very difficult experiments to observe neutrino oscillations are actively pursued in America, Asia, and Europe.

The question about the neutrino mass – either by direct study of the end point of the electron energy spectrum measured in $^3\mathrm{H} \rightarrow {}^3\mathrm{He} + \mathrm{e}^- + \overline{\nu}_\mathrm{e}$ (tritium β-decay) or by observation of neutrino oscillations in terrestrial experiments – still has no definite answer at present.

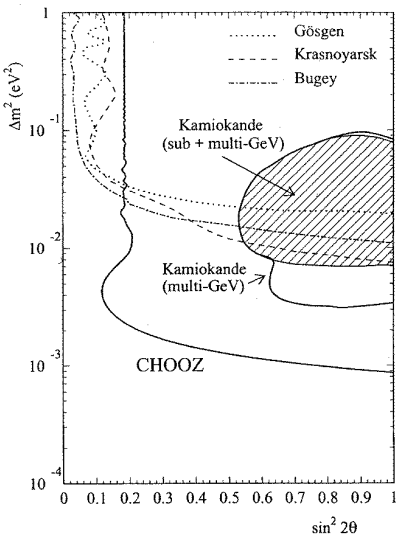

Fig. 12.2. Limits on $\nu_\mathrm{e} \leftrightarrow \nu_\mu$ in the $\sin^2 2\theta$, $|\Delta m^2_{21}|/(eV^2)$ plane from Chooz reactor neutrinos, compared with experiments from Bugey, Gösgen, Krasnoyarsk where the excluded regions are above and to the right of the contours. The allowed area from Kamiokande with atmospheric neutrinos suggests that oscillations might involve tau neutrinos. Courtesy CERN Courier, February 1998

12.3 Oscillations in Matter

In most realistic situations, the neutrinos move not in the vacuum but in matter. For instance, the solar neutrino is produced in the central part of the sun and moves to its surface through the solar material medium. We must therefore consider the effects of the surroundings on the particle oscillations. When a neutrino propagates in a medium filled with other particles, its interaction with matter modifies its oscillations. The reason is that the interaction of the neutrino with matter would change its *effective mass*, just as the well-known example of electromagnetic waves. Massless in vacuum, the photon passes through a medium with a velocity smaller than c, as it gets an effective mass by interacting with matter. In conventional optics, the phenomenon is described by an index of refraction $n \neq 1$ of the medium.

Similarly, as a neutrino goes through matter, its effective mass is modified by its interaction with other particles in the medium. As we will see, since the ν_e interacts with the solar matter differently than ν_μ or ν_τ, the ν_e oscillations in the sun are different from those of the other ν_μ or ν_τ. This

difference causes significant changes in the masses and mixing angles of neutrinos and could give rise to dramatic *resonance oscillations*, known as the Mikheyev–Smirnov–Wolfenstein (MSW) effect.

12.3.1 Index of Refraction, Effective Mass

When a neutrino propagates in matter, its interaction with other particles results in either coherent or incoherent transitions. In a coherent process, the medium remains unchanged, allowing scattered and unscattered neutrino wave functions to interfere. The initial and final states in a scattering in the medium must remain exactly the same, requiring *forward elastic scattering* of neutrinos by particles in the medium. As in conventional optics, these coherent elastic forward scatterings are responsible for optical phenomena and provide effective masses to the neutrinos, as first pointed out by Wolfenstein. On the other hand, any change in the states would produce incoherent waves which cannot give rise to optical phenomena. The index of refraction n in *neutrino optics* may be derived from an effective potential $\mathcal{V}$ that the neutrino 'feels' when it travels in and interacts with the medium. The $\mathcal{V}$ gives masses to the neutrinos and changes their mixing angles. Our purpose is to compute $\mathcal{V}$ and show how the masses of the neutrinos and their mixings in the vacuum are modified by $\mathcal{V}$.

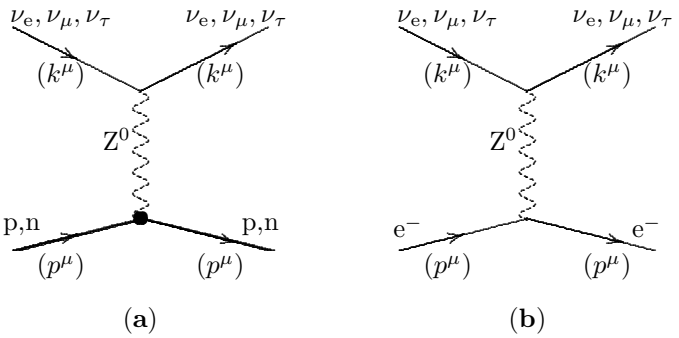

Fig. 12.3. (**a**) Neutrino–proton and neutrino–neutron forward elastic scatterings by Z^0 exchange; (**b**) neutrino–electron forward elastic scatterings by Z^0 exchange

As a specific example, let us consider a neutrino propagating inside the sun, its medium is composed of protons, neutrons, and electrons. We are only interested in elastic scattering of the neutrinos with p , n, and e^- for the reason mentioned above. The Z^0-exchange elastic scatterings of ν_e, ν_μ, ν_τ are identical since there is no difference between the three neutrino families in their interactions with matter by neutral currents (Fig. 12.3). On the other hand, only the ν_e can have an elastic scattering with e^- by the W-exchange charged current $\nu_e + e^- \rightarrow e^- + \nu_e$ (Fig. 12.4). In normal matter like the sun, there are neither muons nor τ leptons, therefore the W-exchange elastic reactions $\nu_\mu + \mu^- \rightarrow \mu^- + \nu_\mu$, $\nu_\tau + \tau^- \rightarrow \tau^- + \nu_\tau$ do not arise for lack of targets

μ^-, τ^-. Inelastic scattering by charged currents $\nu_{\mu,\tau} + \mathrm{e}^- \to (\mu^-, \tau^-) + \nu_\mathrm{e}$ can occur; however these incoherent reactions cannot give rise to optical phenomena responsible for oscillations in matter.

The effective potential is then the sum of $\mathcal{V}_\mathrm{N}$ (from Z^0 exchange) and $\mathcal{V}_\mathrm{C}$ (from W exchange). We first compute $\mathcal{V}_\mathrm{C}$; its important role will become clear later when we discuss the MSW effect. $\mathcal{V}_\mathrm{C}$ is derived from an effective Hamiltonian $H_\mathrm{C}(x)$ built up by charged currents acting in the medium:

$$\begin{aligned}
&\mathcal{V}_\mathrm{C} \equiv \left\langle \nu_\mathrm{e}(k) \left| \int \mathrm{d}^3x H_\mathrm{C}(x) \right| \nu_\mathrm{e}(k) \right\rangle \ , \\
&H_\mathrm{C}(x) = -\mathcal{L}_\mathrm{C}(x) = -\frac{G_\mathrm{F}}{\sqrt{2}} \int \mathrm{d}^3p \ f(E,T) \left\langle e(p) \left| J^\lambda(x) J^\dagger_\lambda(x) \right| e(p) \right\rangle \ , \\
&J^\lambda(x) = \overline{\psi}_\mathrm{e}(x)\gamma^\lambda(1-\gamma_5)\psi_{\nu_\mathrm{e}}(x) \equiv \overline{\psi}_\mathrm{e}(x)\mathcal{O}^\lambda\psi_{\nu_\mathrm{e}}(x) \ . \qquad (12.8)
\end{aligned}$$

The function $f(E,T)$ in (8) is the energy distribution of electrons in the medium at temperature T, normalized to 1, i.e. $\int \mathrm{d}^3p \ f(E,T) = 1$. By Fierz's rearrangement (Appendix):

$$\overline{\psi}_\mathrm{e}(x)\mathcal{O}^\lambda\psi_{\nu_\mathrm{e}}(x) \ \overline{\psi}_{\nu_\mathrm{e}}(x)\mathcal{O}_\lambda\psi_\mathrm{e}(x) = -\overline{\psi}_{\nu_\mathrm{e}}(x)\mathcal{O}^\lambda\psi_{\nu_\mathrm{e}}(x) \ \overline{\psi}_\mathrm{e}(x)\mathcal{O}_\lambda\psi_\mathrm{e}(x) \ ,$$

$$H_\mathrm{C}(x) = \frac{G_\mathrm{F}}{\sqrt{2}}\overline{\psi}_{\nu_\mathrm{e}}(x)\mathcal{O}^\lambda\psi_{\nu_\mathrm{e}}(x) \int \mathrm{d}^3p \ f(E,T) \left\langle e(p) \left| \overline{\psi}_\mathrm{e}(x)\mathcal{O}_\lambda\psi_\mathrm{e}(x) \right| e(p) \right\rangle \ .$$

With the standard normalization of the electron state

$$\psi_\mathrm{e}(x) = \sqrt{\frac{1}{L^3}}\sqrt{\frac{1}{2E}} \ u(p)\mathrm{e}^{-\mathrm{i}px} \quad , \quad \int_{L^3} \mathrm{d}^3x \ \psi^\dagger_\mathrm{e}(x)\psi_\mathrm{e}(x) = 1 \ ,$$

where L^3 is the volume of the box in which the electron state is normalized in the medium, the continuum limit ($L \to \infty$) is obtained by the replacement $1/L^3 \to \mathrm{d}^3p/(2\pi)^3$. We have

$$\begin{aligned}
\left\langle \mathrm{e}^-(p) \left| \overline{\psi}_\mathrm{e}(x)\mathcal{O}_\lambda\psi_\mathrm{e}(x) \right| \mathrm{e}^-(p) \right\rangle &= \frac{1}{2E\langle L^3\rangle}\overline{u}(p)\mathcal{O}_\lambda u(p) \\
&= \frac{1}{2}\frac{\mathrm{Tr}\{(m+\not{p})\mathcal{O}_\lambda\}}{2E\langle L^3\rangle} = N_\mathrm{e}\frac{p_\lambda}{E} \ . \qquad (12.9)
\end{aligned}$$

The factor $\frac{1}{2}$ in the above equation takes care of the spin average of the initial target electron, and $N_\mathrm{e} \equiv 1/\langle L^3\rangle$ is the number of electrons per unit volume (electron number density), which has the dimension of (mass)^3. Since

$$\gamma^\lambda \int \mathrm{d}^3p \ f(E,T) \frac{p_\lambda}{E} = \int \mathrm{d}^3p \ f(E,T) \ \left[\gamma^0 - \frac{\boldsymbol{\gamma}\cdot\boldsymbol{p}}{E}\right] = \gamma^0 \ ,$$

one has for left-handed neutrino $\psi_\mathrm{L}(x)$:

$$H_\mathrm{C} = \frac{G_\mathrm{F}N_\mathrm{e}}{\sqrt{2}}\overline{\psi}_{\nu_\mathrm{e}}(x)\gamma^0(1-\gamma_5)\psi_{\nu_\mathrm{e}}(x) = \sqrt{2} \ G_\mathrm{F} \ N_\mathrm{e} \ \psi^\dagger_\mathrm{L}(x)\psi_\mathrm{L}(x) \ .$$

With $\int \mathrm{d}^3x \left\langle \nu_\mathrm{e} \left| \psi_\mathrm{L}^\dagger(x)\psi_\mathrm{L}(x) \right| \nu_\mathrm{e} \right\rangle = 1$, then using (8), we get

$$\mathcal{V}_\mathrm{C} = \sqrt{2}\, G_\mathrm{F} N_\mathrm{e} \ . \tag{12.10}$$

The potential $\mathcal{V}$ has the dimension of mass, as it should. As we will see later in (12.18), $\mathcal{V}_\mathrm{C}$ is proportional to the amplitude $\mathcal{M}_\mathrm{C}(E_\nu, q^2 = 0)$ of the forward elastic scattering by charged currents $\nu_\mathrm{e}(k) + \mathrm{e}^-(p) \to \nu_\mathrm{e}(k) + \mathrm{e}^-(p)$ (Fig. 12.4) for which the momentum transfer q^2 is zero.

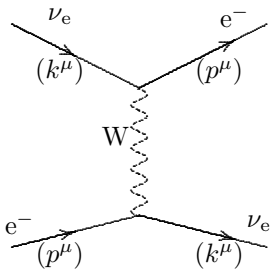

Fig. 12.4. ν_e–e^- forward elastic scatterings by W boson exchange

By the same method, it is a straightforward task to compute $\mathcal{V}_\mathrm{N}$, the potential due to Z^0-exchange contributions. The forward elastic amplitude by neutral currents of Fig. 12.3b is denoted as $\mathcal{M}_\mathrm{N}(E_\nu, q^2 = 0)$. The corresponding effective Hamiltonian $H_\mathrm{N}(x)$ is

$$H_\mathrm{N}(x) = \frac{-G_\mathrm{F}}{\sqrt{2}}\, \overline{\psi}_{\nu_\mathrm{e}}(x)\mathcal{O}^\lambda\psi_{\nu_\mathrm{e}}(x) \int \mathrm{d}^3p\ f(E,T)\ \left\langle \mathrm{e}(p) \left| \overline{\psi}_\mathrm{e}(x)\Gamma_\lambda\psi_\mathrm{e}(x) \right| \mathrm{e}(p) \right\rangle \ ,$$
$$\Gamma_\lambda = \gamma_\lambda(g_\mathrm{V}^\mathrm{e} - \gamma_5 g_\mathrm{A}^\mathrm{e}) \quad , \quad g_\mathrm{V}^\mathrm{e} = -\tfrac{1}{2} + 2\sin^2\theta_\mathrm{W} \ , \ g_\mathrm{A}^\mathrm{e} = -\tfrac{1}{2} \ .$$

The relative sign between the charged current and neutral current amplitudes, $\mathcal{M}_\mathrm{C}$ and $\mathcal{M}_\mathrm{N}$, must be negative, because of the anticommutation relations of the fermionic creation and destruction operators (Sect. 12.4). Since $\mathcal{V}_\mathrm{C}$ and $\mathcal{V}_\mathrm{N}$ are proportional to $\mathcal{M}_\mathrm{C}$ and $\mathcal{M}_\mathrm{N}$ respectively, this relative sign is reflected in $\mathcal{V}_\mathrm{C}$ and $\mathcal{V}_\mathrm{N}$. Taking this minus sign into account, the contribution of the target electron to $\mathcal{V}_\mathrm{N}$ is found to be

$$\mathcal{V}_\mathrm{N}^\mathrm{e} = \frac{-G_\mathrm{F}}{\sqrt{2}}\, (1 - 4\sin^2\theta_\mathrm{W}) N_\mathrm{e} \ . \tag{12.11}$$

For a more general case, we get

$$\mathcal{V}_\mathrm{N} = \sqrt{2}\, G_\mathrm{F} \sum_f \left\{ (T_3^f)_\mathrm{L} - 2\sin^2\theta_\mathrm{W} Q^f \right\} N_f \ .$$

In the case of the sun, the sum over f corresponds to the three targets: p, n, and e^-. With $(T_3^\mathrm{p})_\mathrm{L} = -(T_3^\mathrm{e})_\mathrm{L} = +1/2$, $Q^\mathrm{p} = -Q^\mathrm{e} = +1$, and $N_\mathrm{p} = N_\mathrm{e}$

for an electrically neutral medium, the contributions to $\mathcal{V}_{\rm N}$ from protons and electrons exactly cancel out each other, only those of neutrons remain. With $(T_3^{\rm n})_{\rm L} = -1/2$, $Q^{\rm n} = 0$ and $N_{\rm n}$ is the neutron number density, we get

$$\mathcal{V}_{\rm N} = -(G_{\rm F}/\sqrt{2})N_{\rm n} \; . \tag{12.12}$$

It is instructive to have some numerical values of the number density N for typical media. Since 5.98×10^{23} protons weigh one gram, a ground rock with a density of about $4{\rm g/cm}^3$ has $N_{\rm e} = N_{\rm p} \approx N_{\rm n} \approx (\frac{4}{2}) \times 6 \times 10^{23}/{\rm cm}^3$. The solar core with a density of about $100{\rm g/cm}^3$ has $N_{\rm e} = N_{\rm p} \approx 3N_{\rm n} \approx 75 \times 6 \times 10^{23}/{\rm cm}^3$ (we have neglected the electron mass). Supernova density is about $10^{14}{\rm g/cm}^3$. Also $G_{\rm F}/{\rm cm}^3 \approx 8.96 \times 10^{-38}$ eV $= 4.54 \times 10^{-33}/{\rm cm}$.

One consequence of the potential $\mathcal{V}$ felt by the neutrino traveling in matter is the modification of the relation $E_\nu^2 = |\boldsymbol{p}|^2 + m_\nu^2$ in the vacuum. In matter it reads $E_\nu^2 = |\boldsymbol{p}|^2 + m_\nu^2 + 2|\boldsymbol{p}|\mathcal{V}$ for $|\mathcal{V}| \ll |\boldsymbol{p}|$. We may interpret this modification as an effective mass acquired by the neutrino

$$m_\nu^2 \longrightarrow m_\nu^2 + 2|\boldsymbol{p}|\mathcal{V} \; . \tag{12.13}$$

The index of refraction in the vacuum is

$$n = \frac{|\boldsymbol{p}|}{E_\nu} \approx 1 - \frac{m_\nu^2}{2E_\nu^2} + \cdots \; . \tag{12.14}$$

The propagation of a neutrino in the vacuum has a phase

$$\exp[{\rm i}(n-1)E_\nu t] = \exp\left(-{\rm i}m_\nu^2 t/2E_\nu\right) \; ,$$

which is responsible for oscillations in the vacuum, and (4) is recovered. In a material medium composed of particles – collectively denoted by P – which interact with neutrinos, similar to the conventional photon-optics, the index of refraction is given by

$$n \approx 1 - \frac{m_\nu^2}{2E_\nu^2} + \frac{N_{\rm P}}{4mE_\nu^2}\,\mathcal{M}(E_\nu, q^2 = 0) \; , \tag{12.15}$$

where $\mathcal{M}(E_\nu, q^2 = 0)$ is the dimensionless forward elastic amplitude of the neutrino scattered by the particle P, E_ν is the neutrino energy in the rest frame of P (of mass m), and $N_{\rm P}$ is the number density of P in the medium.

The well-known optical theorem relates the imaginary part of the forward elastic amplitude $\mathcal{M}(E_\nu, q^2 = 0)$ to the total cross-section of the neutrino scattered by P, $\sigma_{\rm tot}(E_\nu)$. According to the theorem [see (15.94)], we have Im $\mathcal{M}(E_\nu, q^2 = 0) = 2m|\boldsymbol{p}|\,\sigma_{\rm tot}(E_\nu) \approx 2mE_\nu\,\sigma_{\rm tot}(E_\nu)$. Note that our definition of amplitudes $\mathcal{M}$ coincides with the amplitudes that enter the general formulas of differential cross-sections given in (4.59) and (4.64). The real and imaginary parts of the index of refraction are

$$\begin{aligned} {\rm Re}\,(n) &\approx 1 - \frac{m_\nu^2}{2E_\nu^2} + \frac{N_{\rm P}}{4mE_\nu^2}\,{\rm Re}\mathcal{M}(E_\nu, q^2 = 0) \; , \\ {\rm Im}\,(n) &\approx \frac{N_{\rm P}}{4mE_\nu^2}\,{\rm Im}\mathcal{M}(E_\nu, q^2 = 0) = \frac{N_{\rm P}}{2E_\nu}\sigma_{\rm tot} = \frac{1}{2\,l\,E_\nu} \; , \end{aligned} \tag{12.16}$$

where l is the mean free path of the neutrino in the medium. On the other hand, from (13), we also have

$$\mathrm{Re}\,(n) \approx 1 - \frac{m_\nu^2 + 2|\boldsymbol{p}|\mathcal{V}}{2E_\nu^2} = 1 - \frac{m_\nu^2}{2E_\nu^2} - \frac{\mathcal{V}}{E_\nu}\,. \tag{12.17}$$

Matching with (16), we get

$$\mathrm{Re}\,\mathcal{M}(E_\nu, q^2 = 0) = \frac{-4mE_\nu}{N_\mathrm{P}}\mathcal{V}\,. \tag{12.18}$$

If the target P is an electron, $\mathcal{V} = \mathcal{V}_\mathrm{C} + \mathcal{V}_\mathrm{N}^\mathrm{e}$, where $\mathcal{V}_\mathrm{C}$ and $\mathcal{V}_\mathrm{N}^\mathrm{e}$ are given by (10) and (11). Putting $m = m_\mathrm{e}$ in the above equation, we obtain the real part of the forward elastic scattering amplitude of ν_e by an electron. It is easy to check, by a direct calculation [see (48) below], that Re $\mathcal{M}_\mathrm{e}(E_\nu, q^2 = 0)$ as given by the Z^0 exchange of Fig. 12.3b and the W exchange of Fig. 12.4 is

$$\mathrm{Re}\,\mathcal{M}_\mathrm{e}(E_\nu, q^2 = 0) = -2\sqrt{2}\,G_\mathrm{F}\,m_\mathrm{e}\,E_\nu\left(1 + 4\sin^2\theta_\mathrm{W}\right) \tag{12.19}$$

and we recover (18).

For the antineutrino, the signs of the forward scattering amplitudes are reversed. Hence in the same medium, the potentials $\mathcal{V}_\mathrm{C}$ and $\mathcal{V}_\mathrm{N}$ felt by the antineutrinos have the opposite sign to the potentials (10) and (12) felt by neutrinos. Once $\mathcal{V}$ is computed, the neutrino effective masses in various media characterized by N_P can be estimated. It is important to note that the oscillation length $\widetilde{L}_\mathrm{osc}$ in matter – related to $\mathcal{V}$ by $\widetilde{L}_\mathrm{osc} \sim 2\pi/\mathcal{V}$ using (6) and (13) – is proportional to G_F^{-1}, whereas the mean free path l depends on $\sigma_\mathrm{tot}^{-1} \sim G_\mathrm{F}^{-2}$. Therefore $\widetilde{L}_\mathrm{osc}$ is many orders of magnitude smaller than l, so that oscillations in matter are in principle accessible.

12.3.2 The MSW Effect

For a quantitative treatment, let us again stick to the simplest case with two flavors ν_e and ν_μ and let us first recapitulate the 2×2 matrix formalism of oscillations in the vacuum suitable for generalization to material medium. The evolution equation of the mass eigenstates ν_1 and ν_2 propagating in the vacuum can be written as

$$\mathrm{i}\frac{\mathrm{d}}{\mathrm{d}t}\begin{pmatrix}\nu_1(t)\\ \nu_2(t)\end{pmatrix} = H\begin{pmatrix}\nu_1(t)\\ \nu_2(t)\end{pmatrix}, \tag{12.20}$$

where H is diagonal in this basis:

$$H = \begin{pmatrix}E_1 & 0\\ 0 & E_2\end{pmatrix} = E_\nu + \begin{pmatrix}m_1^2/2E_\nu & 0\\ 0 & m_2^2/2E_\nu\end{pmatrix}\,. \tag{12.21}$$

Using (1) for the mixing matrix $U(\theta)$ which connects the mass eigenstates ν_1, ν_2 to the flavor physical states $\nu_{\rm e}, \nu_\mu$, we rewrite the above equation as

$$\mathrm{i}\frac{\mathrm{d}}{\mathrm{d}t}\begin{pmatrix}\nu_e(t)\\ \nu_\mu(t)\end{pmatrix} = H'\begin{pmatrix}\nu_e(t)\\ \nu_\mu(t)\end{pmatrix}, \quad \text{where} \quad \Delta \equiv \Delta m^2_{21} = m^2_2 - m^2_1 ,$$
$$H' = U(\theta) H U^\dagger(\theta) = E_\nu + \frac{m^2_1 + m^2_2}{4E_\nu} + \frac{\Delta}{4E_\nu}\begin{pmatrix}-\cos 2\theta & \sin 2\theta\\ \sin 2\theta & \cos 2\theta\end{pmatrix} . \quad (12.22)$$

In terms of the matrix elements H'_{ij}, we write θ, the mixing angle in the vacuum, in the following form, which will be useful later:

$$\tan 2\,\theta = \frac{2\,H'_{21}}{H'_{22} - H'_{11}} . \quad (12.23)$$

We consider now the problem of neutrinos traveling through a material medium. The evolution equation for $\nu_{\rm e}, \nu_\mu$ still keeps the same matrix structure (22), with H' replaced by $\widetilde{H}$,

$$\widetilde{H} = E_\nu + \frac{m^2_1 + m^2_2}{4E_\nu} + \mathcal{V}_{\rm N} + \begin{pmatrix}-\frac{\Delta}{4E_\nu}\cos 2\theta + \mathcal{V}_{\rm C} & \frac{\Delta}{4E_\nu}\sin 2\theta\\ \frac{\Delta}{4E_\nu}\sin 2\theta & \frac{\Delta}{4E_\nu}\cos 2\theta\end{pmatrix} . \quad (12.24)$$

The potential $\mathcal{V}_{\rm N}$ acts on both flavor neutrinos ν_e and ν_μ. It contributes equally to the common effective mass of $\nu_{\rm e}$ and ν_μ through (13). On the other hand, the potential $\mathcal{V}_{\rm C}$ acts only on $\nu_{\rm e}$ and not on ν_μ. Therefore, in the matrix $\widetilde{H}$, $\mathcal{V}_{\rm N}$ is diagonal whereas $\mathcal{V}_{\rm C}$ appears only in $\widetilde{H}_{11}$.

The mixing angle θ in the vacuum now becomes Φ, the mixing angle in matter, using the general formula (23):

$$\tan 2\Phi \equiv \frac{2\widetilde{H}_{21}}{\widetilde{H}_{22} - \widetilde{H}_{11}} = \frac{\Delta \sin 2\theta}{A_{\rm R} - A_{\rm C}} ,$$
$$\text{or} \quad \sin^2 2\Phi = \frac{\tan^2 2\Phi}{1 + \tan^2 2\Phi} = \frac{\Delta^2 \sin^2 2\theta}{(A_{\rm C} - A_{\rm R})^2 + \Delta^2 \sin^2 2\theta} , \quad (12.25)$$

$$\text{where} \quad A_{\rm R} = \Delta \cos 2\theta , \qquad A_{\rm C} = 2E_\nu \mathcal{V}_{\rm C} = 2\sqrt{2} G_{\rm F} N_{\rm e} E_\nu . \quad (12.26)$$

When $N_{\rm e} = 0$, both $\mathcal{V}_{\rm C}$ and $A_{\rm C}$ vanish and Φ is equal to θ as it should be.

The crucial point of (25), first noticed by Mikheyev and Smirnov, is the *resonance behavior* which dramatically changes the mixing angle Φ and reveals unexpected features of the oscillation phenomenon. The angle Φ shown by Fig. 12.5 as a function of $A_{\rm C}$ is clearly a resonance, peaking at the pole $A_{\rm C} = A_{\rm R}$ with a width $\Delta^2 \sin^2 2\theta$.

The sign of $A_{\rm C}$ or $\mathcal{V}_{\rm C}$ is essential for a resonance behavior to appear. With neutrinos, $A_{\rm R}$ and $A_{\rm C}$ have the same signs, and the denominator of (25) could vanish. However, with antineutrinos in the same electron rich medium

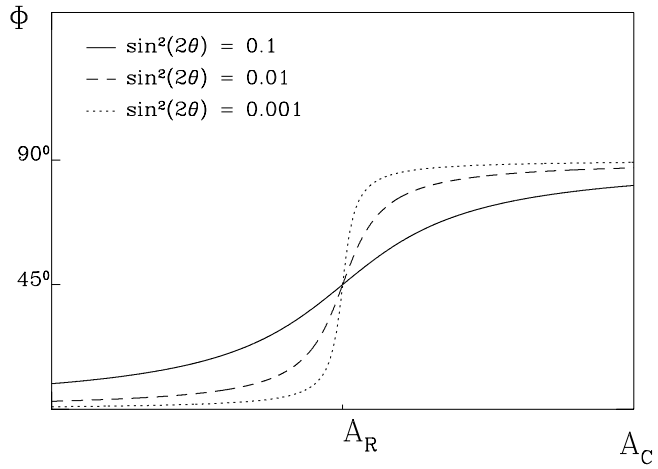

Fig. 12.5. The mixing angle Φ in matter as a function of $A_{\rm C}$

$+A_{\rm C}$ becomes $-A_{\rm C}$ and the resonance behavior is absent. If $A_{\rm C} \approx A_{\rm R}$, then (25) shows that even starting with a very small $\theta \approx 0$ in the vacuum, the mixing angle Φ could become $\approx \pi/4$ in matter. In other words, as soon as it is produced, the neutrino $\nu_{\rm e}$, by its interaction with electrons in matter, becomes equally split into $\nu_{\rm e}$ and ν_μ in the resonance region characterized by $A_{\rm C} \approx A_{\rm R}$. We notice the important role of $A_{\rm C}$ in the MSW effect.

To go further, let us write down the eigenvalues $E_{1,2}$ of $\widetilde{H}$ to understand the exact meaning of this maximum mixing. They are

$$
\begin{aligned}
E_{1,2} &= |\boldsymbol{p}| + \frac{(\mu_{1,2})^2}{2|\boldsymbol{p}|} + \dots \ , \\
(\mu_1)^2 &= \frac{1}{2}\left[m_1^2 + m_2^2 + A_{\rm C} + 2A_{\rm N} - \sqrt{(A_{\rm R} - A_{\rm C})^2 + (\Delta \sin 2\theta)^2}\right] \ , \\
(\mu_2)^2 &= \frac{1}{2}\left[m_1^2 + m_2^2 + A_{\rm C} + 2A_{\rm N} + \sqrt{(A_{\rm R} - A_{\rm C})^2 + (\Delta \sin 2\theta)^2}\right] ,
\end{aligned}
\tag{12.27}
$$

where $A_{\rm N} = 2E_\nu \mathcal{V}_{\rm N} = -\sqrt{2} G_{\rm F} N_{\rm n} E_\nu$. The above formula clearly indicates that even if the neutrinos are massless in the vacuum, i.e. $m_{1,2} = 0$, they can acquire effective masses $\mu_{1,2} \neq 0$ in matter. In the vacuum the relevant quantities are Δ and θ, in matter they become $\widetilde{\Delta}$ and Φ, where $\widetilde{\Delta} = (\mu_2)^2 - (\mu_1)^2 = \sqrt{(A_{\rm R} - A_{\rm C})^2 + (\Delta \sin 2\theta)^2}$, and Φ is given by (25). To illustrate the surprising behavior of neutrino oscillations in matter, let us assume that θ is extremely small, such that in the vacuum, by (1) the light mass eigenstate ν_1 is nearly $\nu_{\rm e}$, and the heavy mass eigenstate ν_2 is almost ν_μ.

In the other extreme condition of matter, we assume that $A_{\rm C} \gg A_{\rm R}$, from (25) the mixing angle $\Phi \approx \pi/2$. Now θ is replaced by Φ, and $\nu_{1,2}$ by $\widetilde{\nu}_{1,2}$ (the mass eigenstates in matter). Since $\nu_{\rm e} = \widetilde{\nu}_1 \ \cos\Phi + \widetilde{\nu}_2 \ \sin\Phi \ \approx \widetilde{\nu}_2$, we

note that ν_e, produced in the region where $A_C \gg A_R$, is nearly a $\widetilde{\nu}_2$ which has an effective mass μ_2 greater than the effective mass μ_1 of ν_μ. The neutrino ν_e which is lighter than the neutrino ν_μ in the vacuum becomes heavier than ν_μ in an electron-rich medium.

In matter where $A_C \gg A_R$, ν_e starts to be a $\widetilde{\nu}_2$, it propagates along the path of the latter (if the adiabatic condition discussed in the following is satisfied). There is not much transition (since the corresponding oscillation length in this region $\widetilde{L}_{osc} \sim 2\pi/\mathcal{V}_C$ is very short) until it arrives in the resonance region ($A_C \sim A_R$) for which $\Phi \approx \pi/4$, the oscillations are enhanced, and $\widetilde{\nu}_2$ is composed of ν_e and ν_μ in equal parts. At the solar surface (i.e. the vacuum), A_C gradually decreases, Φ tends towards θ, $\widetilde{\nu}_2$ gradually becomes $\nu_\mu \cos\theta + \nu_e \sin\theta$, and finally comes out nearly as a ν_μ in the vacuum. The evolution of neutrinos in matter, expressed by (27) and illustrated by Fig. 12.6, is called a *level crossing* : Produced as a ν_e in an electron-dense solar core, the traveling neutrino becomes almost a ν_μ when it reaches the solar surface. The depletion is spectacular indeed.

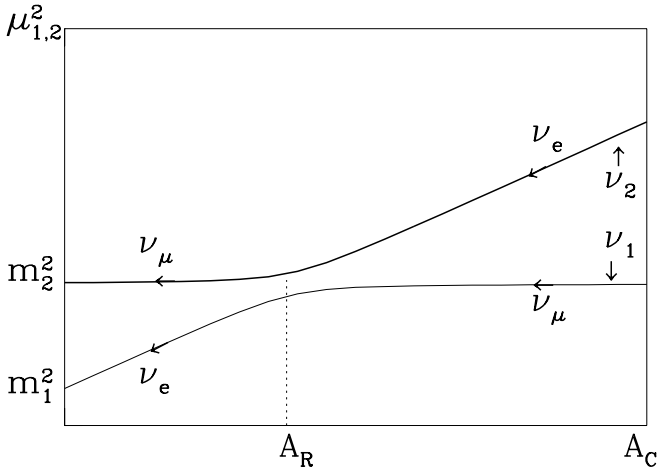

Fig. 12.6. Adiabatic MSW effect: Following the $\widetilde{\nu}_2$ path, a ν_e produced in the solar core becomes a ν_μ at the solar surface

12.3.3 Adiabaticity

So far we have assumed that the solar density N is homogeneous everywhere. It is constant throughout the region covered by the traveling neutrinos. This is actually not the case of the sun, and we must accordingly take into account the variations of $N(r) = N(t)$. We have taken $r = ct = t$ appropriate for relativistic neutrinos, r being the distance from the center of the sun. The mixing angle Φ and the effective masses $\mu_{1,2}$ – given respectively by (25) and (27) – are no longer constant in r, hence in t. The mixing angle in matter, always expressed through its analytic form (25), is now a function

of t since $A_{\rm C}(t)$ depends on it via $N(t)$. First we write $\widetilde{\nu}_1(t)$ and $\widetilde{\nu}_2(t)$, the mass eigenstates in matter, as a mixing of $\nu_{\rm e}$ and ν_μ with the angle $\Phi(t)$,

$$\begin{pmatrix}\widetilde{\nu}_1(t)\\ \widetilde{\nu}_2(t)\end{pmatrix} = \begin{pmatrix}\cos\Phi(t) & -\sin\Phi(t)\\ \sin\Phi(t) & \cos\Phi(t)\end{pmatrix}\begin{pmatrix}\nu_{\rm e}\\ \nu_\mu\end{pmatrix}.$$

In the evolution equation (24) of $\nu_{\rm e}$ and ν_μ, we keep the t dependence of $\mathcal{V}_{\rm C}(t)$. After rewriting $\nu_{\rm e}$ and ν_μ in terms of $\widetilde{\nu}_1$ and $\widetilde{\nu}_2$, we get

$$\mathrm{i}\frac{\mathrm{d}}{\mathrm{d}t}\begin{pmatrix}\widetilde{\nu}_1\\ \widetilde{\nu}_2\end{pmatrix} = \frac{1}{2E_\nu}\begin{pmatrix}\mu_1^2(t) & -\mathrm{i}\delta\mu^2(t)\\ +\mathrm{i}\delta\mu^2(t) & \mu_2^2(t)\end{pmatrix}\begin{pmatrix}\widetilde{\nu}_1\\ \widetilde{\nu}_2\end{pmatrix}, \tag{12.28}$$

where

$$\delta\mu^2(t) = 2E_\nu\frac{\mathrm{d}\Phi(t)}{\mathrm{d}t} = \frac{E_\nu\Delta\sin 2\theta}{[\mu_2^2(t)-\mu_1^2(t)]^2}\left|\frac{1}{N_{\rm e}}\frac{\mathrm{d}N_{\rm e}}{\mathrm{d}t}\right| A_{\rm C}(t)\,. \tag{12.29}$$

The oscillations depend now on an additional parameter denoted by $h(t)$:

$$h(t) \equiv \left|\frac{1}{N_e}\frac{\mathrm{d}N_{\rm e}}{\mathrm{d}t}\right|\,.$$

In general, (28) is solved by numerical methods. We remark that if $N_{\rm e}(t)$ is constant, $\delta\mu^2(t)$ vanishes, and $\widetilde{\nu}_{1,2}$ are stationary states. For a varying density $N(r)$, we can only define the stationary states at a given point r. Nevertheless, if (28) is *almost diagonal*, i.e. if $\delta\mu^2(t) \ll [\mu_2^2(t)-\mu_1^2(t)]$ (a relation referred to as the adiabatic condition), then as long as this condition is satisfied, the matter eigenstates $\widetilde{\nu}_{1,2}$ move in the medium without undergoing transitions between themselves, with the relative admixture of $\nu_{\rm e}, \nu_\mu$ determined according to the value of $N_{\rm e}(r)$ at a given point r. The adiabatic condition can also be rewritten as

$$\frac{\Delta\sin 2\theta}{[\mu_2^2(t)-\mu_1^2(t)]^2}E_\nu\,A_{\rm C}(t)\,h(t) \ll \mu_2^2(t)-\mu_1^2(t)\,. \tag{12.30}$$

In the resonance region where $A_{\rm C} = A_{\rm R} \equiv \Delta\cos 2\theta$, we note from (27) that the right-hand side of the above equation, i.e. $[\mu_2^2-\mu_1^2]$ reaches its minimum value which is equal to $\Delta\sin 2\theta$, whereas the left-hand side is maximum (because $[\mu_2^2-\mu_1^2]$ is now in the denominator). Provided that $h(t)$ is monotonously changing (this is the case of the sun, see below), if (30) is satisfied at the resonance, it is satisfied everywhere. At the resonance, the adiabatic condition (30) becomes

$$\frac{\Delta\sin^2 2\theta}{E_\nu\cos 2\theta} \gg h_{\rm Res}\ ,\ \ h_{\rm Res} = \left|\frac{1}{N_{\rm e}}\frac{\mathrm{d}N_{\rm e}}{\mathrm{d}t}\right|_{\rm Res}\,, \tag{12.31}$$

where $h_{\rm Res}$ is the value of $h(t)$ at the resonance. Physically, the adiabatic condition corresponds to the case of many oscillations that take place in the resonance region. This region is characterized by the resonance oscillation length $\widetilde{L}_{\rm Res} = L_{\rm osc}/\sin 2\theta$, where $L_{\rm osc}$ is given by (6). For the standard solar density, $N_{\rm e}(r) = N_{\rm e}(0){\rm e}^{-ar/R_\odot}$, where $a \simeq 10.54$ and $R_\odot \simeq 7 \times 10^8{\rm m}$ is the radius of the sun, we get $h_{\rm Res} \simeq 3 \times 10^{-15}\,{\rm eV} = 1.52 \times 10^{-10}/{\rm cm}$. When Δ is expressed in $({\rm eV})^2$ and E_ν in MeV, the adiabatic condition (31) is

$$\frac{\sin^2 2\theta(\Delta/{\rm eV}^2)}{\cos 2\theta(E_\nu/{\rm MeV})} \gg 3 \times 10^{-9}\ .$$

If the mixing angle in the vacuum θ satisfies the above inequality, i.e. if (28) is almost diagonal, then for a given E_ν and Δ, the r dependence of $N(r)$ is harmless and the level crossing can be fully achieved. Let us explain in detail the MSW effect in matter satisfying the adiabatic condition. Similar to the vacuum case (3), the amplitude $\widetilde{\mathcal{A}}(\nu_{\rm e} \to \nu_{\rm e}; t)$ in matter is written as

$$\begin{aligned}\widetilde{\mathcal{A}}(\nu_{\rm e} \to \nu_{\rm e}; t) = \sum_{a,b} &\langle \nu_{\rm e}(t)\,|\widetilde{\nu}_b(t)\rangle\,\langle\widetilde{\nu}_b(t)\,|\widetilde{\nu}_b(t_R)\rangle \\ &\times \langle\widetilde{\nu}_b(t_R)\,|\widetilde{\nu}_a(t_R)\rangle\,\langle\widetilde{\nu}_a(t_R)\,|\widetilde{\nu}_a(t_0)\rangle\,\langle\widetilde{\nu}_a(t_0)\,|\nu_{\rm e}(t_0)\rangle\ , \quad (12.32)\end{aligned}$$

where t_0 and t_R are the traveling time (or distance) from the solar center to the $\nu_{\rm e}$ production region and to the resonance localization respectively, and reading from right to left, the first term is

$$\langle\widetilde{\nu}_a(t_0)\,|\nu_{\rm e}(t_0)\rangle = U^*_{{\rm e}a}(\Phi)\ ,$$

where U is the mixing matrix in matter with the angle Φ, similar to (1) in the vacuum. To simplify, we consider only the two-family case ($a, b = 1, 2$). Under the adiabatic condition, the stationary mass-eigenstates $\widetilde{\nu}_1$, $\widetilde{\nu}_2$ propagate from the core to the surface without mixing, i.e. $\widetilde{\nu}_1$ remains $\widetilde{\nu}_1$, and $\widetilde{\nu}_2$ remains $\widetilde{\nu}_2$ in the whole distance covered. Then the three factors in the middle of (32) are simply

$$\begin{aligned}&\langle\widetilde{\nu}_b(t)\,|\widetilde{\nu}_b(t_R)\rangle\,\langle\widetilde{\nu}_b(t_R)\,|\widetilde{\nu}_a(t_R)\rangle\,\langle\widetilde{\nu}_a(t_R)\,|\widetilde{\nu}_a(t_0)\rangle \\ &\qquad = \delta_{ab}\exp[{\rm i}\int_{t_0}^{t} E_a(t'){\rm d}t'] \equiv \delta_{ab}\exp[{\rm i}\,E_a(t)/E]\ .\end{aligned}$$

Note that $E_a(t)$ is a function of time (or distance) because the effective mass μ_a given by (27) changes as it propagates in matter (Fig. 12.6). The factor $\langle\nu_{\rm e}(t)\,|\widetilde{\nu}_b(t)\rangle$ in the extreme left of the right-hand side of (32) which projects out $\nu_{\rm e}$ from $\widetilde{\nu}_b$ with the mixing angle θ in the vacuum is

$$\langle\nu_{\rm e}(t)\,|\widetilde{\nu}_b(t)\rangle = U_{{\rm e}b}(\theta)\ .$$

The transition probability becomes

$$\widetilde{P}(\nu_{\rm e}\to\nu_{\rm e},t)=\left|\sum_{a=1,2}U_{{\rm e}a}(\theta)U^*_{{\rm e}a}(\Phi)\exp\left[\frac{-{\rm i}E_a(t)}{2E}\right]\right|^2$$

$$=\cos^2\theta\,\cos^2\Phi+\sin^2\theta\,\sin^2\Phi+\tfrac{1}{2}\sin 2\theta\,\sin 2\Phi\cos\frac{\widetilde{\delta}(t)}{2E}\,,$$

$$\widetilde{\delta}(t)=\int_{t_0}^{t}{\rm d}t'[\mu_2^2(t')-\mu_1^2(t')]=\int_{t_0}^{t}{\rm d}t'\sqrt{[\Delta\cos 2\theta-A_{\rm C}(t')]^2+(\Delta\sin 2\theta)^2}\,.$$

In practice, the oscillating term that depends on t can be neglected, and the time average of $\widetilde{P}(\nu_{\rm e}\to\nu_{\rm e},t)$ is

$$\widetilde{P}(\nu_{\rm e}\to\nu_{\rm e})=\cos^2\theta\,\cos^2\Phi+\sin^2\theta\,\sin^2\Phi\,.$$

Since Φ depends on $A_{\rm C}$, $\widetilde{P}(\nu_{\rm e}\to\nu_{\rm e})$ is a function of the localization where neutrinos are produced. When they are produced in the region $A_{\rm C}\gg A_{\rm R}$, $\Phi\approx 90^0$, we get $\widetilde{P}(\nu_{\rm e}\to\nu_{\rm e})=\sin^2\theta$, so that depending on the value of θ in the vacuum, we can have any amount of depletion. Figure 12.6 illustrates the situation. This is in sharp contrast to the vacuum depletion given by (4), where $P(\nu_{\rm e}\to\nu_{\rm e})=\cos^4\theta+\sin^4\theta=1-\frac{1}{2}\sin^2 2\theta$ is larger than $\frac{1}{2}$ for all θ.

Summary. The nonzero mass of neutrinos is of great importance not only in particle physics but also in astrophysics and cosmology. If the three neutrino families have nondegenerate masses, they could mix together like the quark families and oscillations would occur. The answer to the question on the existence of neutrino masses depends mainly on possible observations of oscillations either in the vacuum or in a material medium. This may be the only experimental method to measure their vanishingly small masses. To cover the large spectrum of Δm^2 between 10^{-12} to $10^3\,{\rm eV}^2$ (see Table 12.1), several sources of neutrino production should be exploited. From the sun to the particle accelerators and nuclear reactors, each source – with its specific energy and distance to the detectors – brings an answer appropriate to each range of values of Δm^2. Finally, the solar neutrino deficit may find its explanation in the MSW mechanism.

12.4 Neutral Currents by Neutrino Scattering

We recall that weak interactions were historically discovered by processes involving charged currents, their first manifestation at the beginning of the century was the β-radioactivity of nuclei for which the neutron disintegration ${\rm n}\to{\rm p}+{\rm e}^-+\overline{\nu}_{\rm e}$ represents the simplest mode. The amplitude of this decay is obtained from the product of two charged currents: the hadronic one $V_{\rm ud}\overline{u}\gamma_\mu(1-\gamma_5)d$ which may be written as a ${\rm d}\to{\rm u}$ transition between the quark u , d fields connected by the CKM matrix element $V_{\rm ud}$, and the leptonic one $\overline{e}\gamma^\mu(1-\gamma_5)\nu_{\rm e}$ constructed from the ${\rm e}^-$ and $\nu_{\rm e}$ fields. All charged

currents share the universal V − A property symbolized by $\gamma_\mu(1-\gamma_5)$. There are in all $9 = 3 \times 3$ hadronic charged currents, only in this specific d → u transition is flavor conserved.

12.4.1 Neutral Currents, Why Not?

From the beginning of the β-radioactivity period to the formulation of the standard model (SM) in the 1970s, physicists had always wondered why only charged currents are involved in weak interactions and not neutral currents, since *a priori* there is no deep reason to suppress the latter. Moreover, in every non-Abelian gauge theory that may underlie weak interactions – the SM is a prototype – the neutral currents (NC) naturally emerge on an equal footing with the charged currents (CC). The problem is to demonstrate experimentally the existence of the neutral currents.

We illustrate the situation by an example. The hadronic charged currents $V_{\rm ud}\overline{u}\gamma_\mu(1-\gamma_5)d$ and $V_{\rm us}\overline{u}\gamma_\mu(1-\gamma_5)s$ are respectively responsible for the decays $\pi^+ \to {\rm e}^+ + \nu_{\rm e}$ and $\mathrm{K}^+ \to \mu^+ + \nu_\mu$ (Fig. 12.7). If the hadronic neutral and charged currents have comparable couplings, as they do in the case of non-Abelian gauge theories, we would expect that $\Gamma(\pi^0 \to {\rm e}^+ + {\rm e}^-) \approx \Gamma(\pi^+ \to {\rm e}^+ + \nu_{\rm e})$ and $\Gamma(\mathrm{K}^0 \to \mu^+ + \mu^-) \approx \Gamma(\mathrm{K}^+ \to \mu^+ + \nu_\mu)$. But nothing of the kind happens for the latter case, the rate $\Gamma(\mathrm{K}^0_{\rm L} \to \mu^+ + \mu^-)$ is very suppressed, being $\approx 2.72 \times 10^{-9}\ \Gamma(\mathrm{K}^+ \to \mu^+ + \nu_\mu)$. Another example of the strongly suppressed strangeness-changing neutral current is the rate of $\mathrm{K}^+ \to \pi^+ + {\rm e}^+ + {\rm e}^-$, which is much weaker than the rate of strangeness-changing charged current involved in $\mathrm{K}^+ \to \pi^0 + {\rm e}^+ + \nu_{\rm e}$ (Sect. 7.6). Obviously, there must exist a cancelation mechanism that *forbids strangeness-changing neutral current*, and at the same time *allows strangeness-changing charged current*. As explained in Chap. 9, these two constraints are realized by the Glashow–Iliopoulos–Maiani (GIM) mechanism, via the unitarity of the Cabibbo–Kobayashi–Maskawa (CKM) matrix. At the lowest order $G_{\rm F}$ tree-diagram level, flavors (strangeness, charm, bottom, top) are systematically conserved in neutral currents but generally not in charged currents.

The absence of $\mathrm{K}^0_{\rm L} \to \mu^+ + \mu^-$ at the tree diagram level is illustrated by Fig. 12.8b. The amplitudes of all flavor-changing neutral currents (FCNC) can only come from loop diagrams similar to the penguin loop considered in Chap. 11 where the gluon is replaced by the photon or the Z^0. Compared to the charged current tree amplitude of order $G_{\rm F}$, these FCNC loop amplitudes are of the order of $G_{\rm F}\alpha_{\rm em}/\pi$, its computation is similar to (11.94).

But how about $\pi^0 \to {\rm e}^+ + {\rm e}^-$, the flavor-conserving neutral current process (Fig. 12.8a) which can occur at the tree level ? Unsuppressed by GIM, its weak decay rate could be similar to the usual $\pi^+ \to {\rm e}^+ + \nu_{\rm e}$. The reason why the existence of neutral currents was not suspected and the $\pi^0 \to {\rm e}^+ + {\rm e}^-$ mode – a typical manifestation of neutral current – was not actively searched for, is simply that electromagnetic interactions also govern this decay through the chain $\pi^0 \to \gamma + \gamma \to {\rm e}^+ + {\rm e}^-$. This electromagnetic transition dominates

the weak decay $\pi^0 \to Z^0 \to e^+ + e^-$ by many orders of magnitude (Problem 12.4). Therefore $\pi^0 \to e^+ + e^-$, contaminated by electromagnetic interactions, is not a clean process for proving the existence of neutral currents.

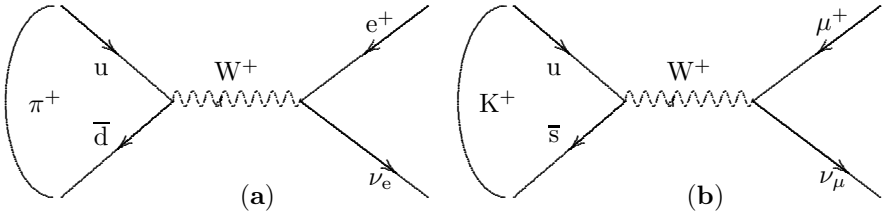

Fig. 12.7. Decays by charged currents: (**a**) $\pi^+ \to e^+ + \nu_e$; (**b**) $K^+ \to \mu^+ + \nu_\mu$

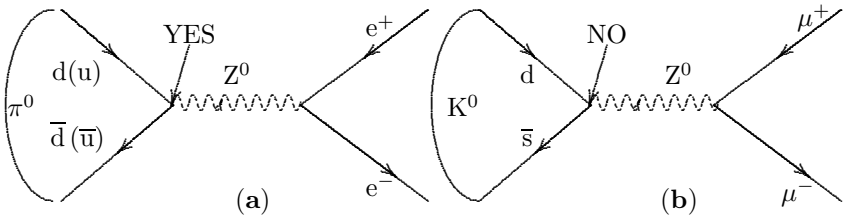

Fig. 12.8. Decays by neutral currents: (**a**) $\pi^0 \to e^+ + e^-$ flavor-conserving neutral current is allowed; (**b**) $K^0 \to \mu^+ + \mu^-$ flavor-changing neutral current is forbidden

From these considerations, we learn that at low energies, electromagnetic processes always dominate weak neutral current ones. For the latter to show up, one should consider reactions in which electromagnetic interactions are absent. We come to the crucial role of neutrinos in the discovery of weak neutral currents which consecrates the standard model. Since neutrinos are insensitive to electromagnetic forces, it suffices to observe the absence of charged leptons in neutrino scatterings to prove the existence of neutral currents. For example, $\nu_e + n \to e^- + p$ is due to charged currents but $\nu_e + p \to \nu_e + p$ can only come from neutral currents. More generally, in the scattering of neutrinos by a target T, if the cross-section $\sigma(\nu_\ell + T \to$ *without* $\ell^- + \cdots)$ is comparable to $\sigma(\nu_\ell + T \to$ *with* $\ell^- + \cdots)$, then the existence of neutral currents is irrefutable. It was precisely how the latter were discovered at CERN by the Gargamelle collaboration in 1973, ten years before the neutral current carrier Z^0 was found at CERN and SLAC.

12.4.2 Neutrino–Electron Scattering

The scattering of neutrino by electron, a purely leptonic reaction, is difficult to observe since the cross-section, being proportional to the electron mass, is small ($\sigma \simeq 10^{-42}\text{cm}^2$). This experimental difficulty is compensated by clean

theoretical treatments, since with pointlike leptons, theoretical treatments do not suffer from uncertainties due to weak form factors inherent to hadrons. From the neutrino–electron scattering, one can deduce the neutral-current properties, the Weinberg angle $\theta_{\rm W}$, and the $\rm W^{\pm}$ and $\rm Z^0$ masses.

We consider the following reactions:

$$\nu_\mu + \mathrm{e}^- \to \nu_\mu + \mathrm{e}^- \quad , \quad \overline{\nu}_\mu + \mathrm{e}^- \to \overline{\nu}_\mu + \mathrm{e}^- \ , \tag{I}$$

$$\nu_\mathrm{e} + \mathrm{e}^- \to \nu_\mathrm{e} + \mathrm{e}^- \quad , \quad \overline{\nu}_\mathrm{e} + \mathrm{e}^- \to \overline{\nu}_\mathrm{e} + \mathrm{e}^- \ , \tag{II}$$

$$\nu_\mu + \mathrm{e}^- \to \mu^- + \nu_\mathrm{e} \ . \tag{III}$$

The reactions (I) are governed only by neutral currents (NC), in (III) are involved charged currents (CC), while both NC and CC participate in (II). The sources of $\overline{\nu}_\mathrm{e}$ are mainly from nuclear reactors, their energies are in the MeV range, while the $\nu_\mu, \overline{\nu}_\mu$ mainly come from the decays of π and K mesons produced by accelerators. Their energies can reach a few hundred GeV.

We start with the pure NC reaction $\nu_\mu(k_1) + \mathrm{e}^-(p_1) \to \nu_\mu(k_2) + \mathrm{e}^-(p_2)$; the corresponding Feynman diagram is similar to Fig. 12.3b. For non-forward scattering considered here, $k_1 \neq k_2$ and $p_1 \neq p_2$. The kinematics of two-body $\to$ two-body reactions is conveniently described by the Mandelstam variables

$$\begin{aligned} s &\equiv (k_1 + p_1)^2 = (k_2 + p_2)^2 \ , \\ t &\equiv (k_1 - k_2)^2 = (p_2 - p_1)^2 \ , \\ u &\equiv (k_1 - p_2)^2 = (k_2 - p_1)^2 \ , \end{aligned} \tag{12.33}$$

only two of which are independent since $s + t + u = \Sigma_j m_j^2 = 2m_\mathrm{e}^2 + 2m_\nu^2$. In the following, we take $m_\nu = 0$ and put $m_\mathrm{e} = m$.

In the center-of-mass system $\boldsymbol{k}_1 + \boldsymbol{p}_1 = \boldsymbol{0} = \boldsymbol{k}_2 + \boldsymbol{p}_2$, and $\boldsymbol{k}_1 \cdot \boldsymbol{k}_2 = |\boldsymbol{k}_1||\boldsymbol{k}_2| \cos\theta_{\rm cm}$, $\sqrt{s}$ is the total energy of the ingoing (or outgoing) particles, and $|\boldsymbol{k}_1| = |\boldsymbol{k}_2| = (s - m^2)/2\sqrt{s}$. The momentum transfer is denoted by $q_\mu = (k_1 - k_2)_\mu$, such that $t = q^2 = -|\boldsymbol{k}_1 - \boldsymbol{k}_2|^2$. We also write $Q^2 = -q^2 \geq 0$.

In the laboratory system for which the target electron is at rest, $\boldsymbol{p}_1 = \boldsymbol{0}$, we have $s = m^2 + 2mE_\nu$ where E_ν is the incoming neutrino energy, and $t = -2m(E_\mathrm{e} - m) = -2mT_\mathrm{e}$. E_e is the outgoing electron energy. Another laboratory variable frequently used is $y \equiv T_\mathrm{e}/E_\nu = -t/(s - m^2)$. The following relations may be useful :

$$\begin{aligned} &k_1 \cdot p_2 = k_2 \cdot p_1 = m(m + E_\nu - E_\mathrm{e}) = mE_\nu(1 - y) = (s + t - m^2)/2 \ , \\ &k_1 \cdot p_1 = k_2 \cdot p_2 = mE_\nu = (s - m^2)/2 \ , \ \ k_1 \cdot k_2 = -t/2 \ , \\ &Q^2 = 2mE_\nu\, y \quad ; \quad 0 \leq Q^2 \leq (s - m^2)^2/s \ ; \ 0 \leq y \leq 1 - m^2/s \ . \end{aligned} \tag{12.34}$$

The two-body $\to$ two-body cross-section always depends on two independent variables that can be chosen as s and t, or E_ν and y in the laboratory frame, or $\sqrt{s}$ and $\theta_{\rm cm}$ in the center-of-mass system. Using the general formulas

(4.59) and (4.62), we have

$$\frac{\mathrm{d}\sigma}{\mathrm{d}\cos\theta_{\rm cm}} = \frac{1}{32\pi\ s}\Big(\tfrac{1}{2}\sum_{\rm spin}|\mathcal{M}_{\rm Z}|^2\Big)\ ,$$
$$\frac{\mathrm{d}\sigma}{\mathrm{d}Q^2} = \frac{1}{16\pi\,(s-m^2)^2}\Big(\tfrac{1}{2}\sum_{\rm spin}|\mathcal{M}_{\rm Z}|^2\Big)\ . \tag{12.35}$$

The symbol $\frac{1}{2}\sum_{\rm spin}$ refers to the averaging over the incoming electron spins, since it is unnecessary to do spin averaging for the incoming left-handed neutrino which has only one helicity. The amplitude of $\nu_\mu(k_1)+\mathrm{e}^-(p_1)\to\nu_\mu(k_2)+\mathrm{e}^-(p_2)$ obtained from the Feynman rules is

$$\begin{aligned}\mathcal{M}_{\rm Z} &= \mathrm{i}\left(\frac{-\mathrm{i}g}{2\sqrt{2}\cos\theta_{\rm W}}\right)^2\overline{u}(k_2)\gamma^\mu(1-\gamma_5)u(k_1)\\ &\quad\times\frac{-\mathrm{i}(g_{\mu\nu}-q_\mu q_\nu/M_{\rm Z}^2)}{q^2-M_{\rm Z}^2}\,\overline{u}(p_2)\gamma^\nu(g_{\rm V}^{\rm e}-g_{\rm A}^{\rm e}\gamma_5)u(p_1)\\ g_{\rm V}^{\rm e} &= -\tfrac{1}{2}+2\sin^2\theta_{\rm W}\ ;\qquad g_{\rm A}^{\rm e}=-\tfrac{1}{2}\ .\end{aligned} \tag{12.36}$$

The product $q_\mu\,\overline{u}(k_2)\gamma^\mu(1-\gamma_5)u(k_1)$ vanishes with massless neutrinos, leaving only the $g_{\mu\nu}$ to the Z^0 propagator. With $G_{\rm F}/\sqrt{2}=g^2/8M_{\rm Z}^2\cos^2\theta_{\rm W}$,

$$\mathcal{M}_{\rm Z} = \frac{G_{\rm F}}{\sqrt{2}}\frac{\overline{u}(k_2)\gamma^\mu(1-\gamma_5)u(k_1)\ \overline{u}(p_2)\gamma_\mu(g_{\rm V}^{\rm e}-g_{\rm A}^{\rm e}\gamma_5)u(p_1)}{(1+Q^2/M_{\rm Z}^2)}\ , \tag{12.37}$$

so that

$$\tfrac{1}{2}\sum_{\rm spin}|\mathcal{M}_{\rm Z}|^2 = \frac{G_{\rm F}^2}{2(1+Q^2/M_{\rm Z}^2)^2}\ \big(\tfrac{1}{2}A_{\mu\rho}\ B^{\mu\rho}\big)\ ,$$

$$\begin{aligned}A_{\mu\rho} &= \sum_{\rm spin}\overline{u}(p_2)\gamma_\mu(g_{\rm V}^{\rm e}-g_{\rm A}^{\rm e}\gamma_5)u(p_1)\ \overline{u}(p_1)\gamma_\rho(g_{\rm V}^{\rm e}-g_{\rm A}^{\rm e}\gamma_5)u(p_2)\\ &= \mathrm{Tr}\left[\not{p}_2\gamma_\mu\not{p}_1\gamma_\rho[(g_{\rm V}^{\rm e})^2+(g_{\rm A}^{\rm e})^2-2g_{\rm V}^{\rm e}g_{\rm A}^{\rm e}\gamma_5]+m^2[(g_{\rm V}^{\rm e})^2-(g_{\rm A}^{\rm e})^2]\gamma_\mu\gamma_\rho\right],\\ B^{\mu\rho} &= \sum_{\rm spin}\overline{u}(k_2)\gamma^\mu(1-\gamma_5)u(k_1)\ \overline{u}(k_1)\gamma^\rho(1-\gamma_5)u(k_2)\\ &= 2\ \mathrm{Tr}\left[\not{k}_2\gamma^\mu\not{k}_1\gamma^\rho(1-\gamma_5)\right]\ .\end{aligned} \tag{12.38}$$

Using the relation

$$\begin{aligned}&\mathrm{Tr}[\gamma^\lambda\gamma^\mu\gamma^\sigma\gamma^\rho(a-b\gamma_5)]\times\mathrm{Tr}[\gamma_\alpha\gamma_\mu\gamma_\beta\gamma_\rho(c-d\gamma_5)]\\ &=32\ [ac(\delta_\alpha^\lambda\delta_\beta^\sigma+\delta_\alpha^\sigma\delta_\beta^\lambda)+bd(\delta_\alpha^\lambda\delta_\beta^\sigma-\delta_\alpha^\sigma\delta_\beta^\lambda)]\ ,\end{aligned} \tag{12.39}$$

we obtain

$$\begin{aligned}A_{\mu\rho}\ B^{\mu\rho} &= 64\ \big[(g_{\rm V}^{\rm e}+g_{\rm A}^{\rm e})^2(k_1\cdot p_1)(k_2\cdot p_2)\\ &\quad+(g_{\rm V}^{\rm e}-g_{\rm A}^{\rm e})^2(k_1\cdot p_2)(k_2\cdot p_1)+[(g_{\rm A}^{\rm e})^2-(g_{\rm V}^{\rm e})^2]m^2(k_1\cdot k_2)\big]\ .\end{aligned} \tag{12.40}$$

Putting (40) into (34), (35), and (38), we have

$$\frac{\mathrm{d}\sigma(\nu_\mu + \mathrm{e}^- \to \nu_\mu + \mathrm{e}^-)}{\mathrm{d}Q^2} = \frac{G_\mathrm{F}^2}{4\pi(s-m^2)^2}\,\frac{1}{(1+Q^2/M_\mathrm{Z}^2)^2}\times \tag{12.41}$$
$$\left[(g_\mathrm{V}^\mathrm{e}+g_\mathrm{A}^\mathrm{e})^2(s-m^2)^2 + (g_\mathrm{V}^\mathrm{e}-g_\mathrm{A}^\mathrm{e})^2(s-m^2-Q^2)^2 + 2[(g_\mathrm{A}^\mathrm{e})^2-(g_\mathrm{V}^\mathrm{e})^2]m^2Q^2\right]\ .$$

Neglecting $m^2 \ll s, Q^2$, the integrated cross-section becomes

$$\sigma \equiv \int_0^s \frac{\mathrm{d}\sigma}{\mathrm{d}Q^2}dQ^2 = \frac{G_\mathrm{F}^2\,s}{4\pi}\left\{\frac{(g_\mathrm{V}^\mathrm{e}+g_\mathrm{A}^\mathrm{e})^2}{(1+s/M_\mathrm{Z}^2)} + \right. \tag{12.42}$$
$$\left. + (g_\mathrm{V}^\mathrm{e}-g_\mathrm{A}^\mathrm{e})^2\frac{M_\mathrm{Z}^2}{s}\left[1+\frac{2M_\mathrm{Z}^2}{s}-\frac{2M_\mathrm{Z}^2}{s}\left(1+\frac{M_\mathrm{Z}^2}{s}\right)\log\left(1+\frac{s}{M_\mathrm{Z}^2}\right)\right]\right\}.$$

For $s \ll M_\mathrm{Z}^2$, we develop the logarithm term of (42) in powers of s/M_Z^2, then in the first approximation, the cross-section depends linearly on s:

$$\sigma(\nu_\mu + \mathrm{e}^- \to \nu_\mu + \mathrm{e}^-) \approx \frac{G_\mathrm{F}^2\,s}{4\pi}\left[(g_\mathrm{V}^\mathrm{e}+g_\mathrm{A}^\mathrm{e})^2 + \frac{1}{3}(g_\mathrm{V}^\mathrm{e}-g_\mathrm{A}^\mathrm{e})^2\right]\ . \tag{12.43}$$

The Z^0 propagator effect through $(1+Q^2/M_\mathrm{Z}^2)^{-2}$ in (41) is very important at high energies, since for $s \gg M_\mathrm{Z}^2$, the cross-section (42) ceases to increase with s, it bends down and tends asymptotically towards a constant

$$\lim_{s\to\infty}\sigma(\nu_\mu + \mathrm{e}^- \to \nu_\mu + \mathrm{e}^-) = \frac{G_\mathrm{F}^2 M_\mathrm{Z}^2}{2\pi}[(g_\mathrm{V}^\mathrm{e})^2 + (g_\mathrm{A}^\mathrm{e})^2]\,. \tag{12.44}$$

The physical significance of (43) and (44) is worth emphasizing. A cross-section cannot increase forever as a linear function of energy without violating the unitarity of the S-matrix. Based on the most general properties of the latter, Froissart and Martin show that a total cross-section – hence *a fortiori* an elastic cross-section considered here – cannot grow asymptotically faster than $(\log s)^2$. At low energies, the linear dependence of (43) on s is only approximate; actually, at high energies the cross-section (44) tends to a constant in accordance with the asymptotic theorem (Froissart bound).

In the laboratory frame, at low energy $mE_\nu \ll M_\mathrm{Z}^2$, we neglect Q^2/M_Z^2 and use (34), then (41) and (43) can be written as

$$\frac{\mathrm{d}\sigma(\nu_\mu + \mathrm{e}^- \to \nu_\mu + \mathrm{e}^-)}{\mathrm{d}y} = \frac{G_\mathrm{F}^2 mE_\nu}{2\pi}\left[(g_\mathrm{V}^\mathrm{e}+g_\mathrm{A}^\mathrm{e})^2 + (g_\mathrm{V}^\mathrm{e}-g_\mathrm{A}^\mathrm{e})^2(1-y)^2\right]\ ,$$

$$\sigma(\nu_\mu + \mathrm{e}^- \to \nu_\mu + \mathrm{e}^-) = \frac{G_\mathrm{F}^2 mE_\nu}{2\pi}\left[(g_\mathrm{V}^\mathrm{e}+g_\mathrm{A}^\mathrm{e})^2 + \tfrac{1}{3}(g_\mathrm{V}^\mathrm{e}-g_\mathrm{A}^\mathrm{e})^2\right]\ . \tag{12.45}$$

The y distribution as well as the integrated cross-section enable us to extract $g_\mathrm{V}^\mathrm{e}, g_\mathrm{A}^\mathrm{e}$, i.e. $\sin^2\theta_\mathrm{W}$.

For the antineutrino $\overline{\nu}_\mu$ scattering $\overline{\nu}_\mu(k_1) + \mathrm{e}^-(p_1) \to \overline{\nu}_\mu(k_2) + \mathrm{e}^-(p_2)$, its cross-section can be deduced from $\nu_\mu(k_1) + \mathrm{e}^-(p_1) \to \nu_\mu(k_2) + \mathrm{e}^-(p_2)$ by a simple substitution $g_{\mathrm{R}}^2 \equiv (g_{\mathrm{V}}^{\mathrm{e}} + g_{\mathrm{A}}^{\mathrm{e}})^2 \leftrightarrow g_{\mathrm{L}}^2 \equiv (g_{\mathrm{V}}^{\mathrm{e}} - g_{\mathrm{A}}^{\mathrm{e}})^2$. This rule can be traced back to (37) for which the current $\overline{u}(k_2)\gamma^\lambda(1-\gamma_5)u(k_1)$ is replaced by $\overline{v}(k_1)\gamma^\lambda(1-\gamma_5)v(k_2)$, i.e. $k_1 \leftrightarrow k_2$, and the substitution $g_R^2 \leftrightarrow g_L^2$ comes from (40) in which the last term proportional to m^2 is neglected. Thus

$$\frac{\mathrm{d}\sigma(\overline{\nu}_\mu + \mathrm{e}^- \to \overline{\nu}_\mu + \mathrm{e}^-)}{\mathrm{d}y} = \frac{G_{\mathrm{F}}^2 m E_{\overline{\nu}}}{2\pi}\left[(g_{\mathrm{V}}^{\mathrm{e}} - g_{\mathrm{A}}^{\mathrm{e}})^2 + (g_{\mathrm{V}}^{\mathrm{e}} + g_{\mathrm{A}}^{\mathrm{e}})^2(1-y)^2\right] ,$$

$$\sigma(\overline{\nu}_\mu + \mathrm{e}^- \to \overline{\nu}_\mu + \mathrm{e}^-) = \frac{G_{\mathrm{F}}^2 m E_{\overline{\nu}}}{2\pi}\left[(g_{\mathrm{V}}^{\mathrm{e}} - g_{\mathrm{A}}^{\mathrm{e}})^2 + \tfrac{1}{3}(g_{\mathrm{V}}^{\mathrm{e}} + g_{\mathrm{A}}^{\mathrm{e}})^2\right] . \quad (12.46)$$

Numerically, with $G_{\mathrm{F}}^2 m_{\mathrm{e}} E_\nu = 27.05 \times 10^{-42}\mathrm{cm}^2 (E_\nu/\ \mathrm{GeV})$, we get

$$\sigma(\nu_\mu + \mathrm{e}^- \to \nu_\mu + \mathrm{e}^-) = 4.3\,\frac{E_\nu}{\mathrm{GeV}}\left[(2\sin^2\theta_{\mathrm{W}} - 1)^2 + \tfrac{4}{3}\sin^4\theta_{\mathrm{W}}\right]\ 10^{-42}\mathrm{cm}^2,$$

$$\sigma(\overline{\nu}_\mu + \mathrm{e}^- \to \overline{\nu}_\mu + \mathrm{e}^-) = 4.3\,\frac{E_{\overline{\nu}}}{\mathrm{GeV}}\left[4\sin^4\theta_{\mathrm{W}} + \tfrac{1}{3}(2\sin^2\theta_{\mathrm{W}} - 1)^2\right]\ 10^{-42}\mathrm{cm}^2.$$

The ratio of the neutrino/antineutrino cross-sections, which is given by

$$R_{\mathrm{N}} \equiv \frac{\sigma(\nu_\mu + \mathrm{e}^- \to \nu_\mu + \mathrm{e}^-)}{\sigma(\overline{\nu}_\mu + \mathrm{e}^- \to \overline{\nu}_\mu + \mathrm{e}^-)} = 3\,\frac{1 - 4\sin^2\theta_{\mathrm{W}} + \frac{16}{3}\sin^4\theta_{\mathrm{W}}}{1 - 4\sin^2\theta_{\mathrm{W}} + 16\sin^4\theta_{\mathrm{W}}} ,$$

enables us to extract $\sin^2\theta_{\mathrm{W}}$. By this method, the electron detection efficiencies cancel in the ratio, and an absolute neutrino flux is not needed. Systematic errors are significantly reduced, resulting in an improvement of the determination of $\sin^2\theta_{\mathrm{W}} = 0.211 \pm 0.036 \pm 0.011$. From (44) and the rule $g_{\mathrm{L}}^2 \leftrightarrow g_{\mathrm{R}}^2$ for $\nu \leftrightarrow \overline{\nu}$, the ratio R_{N} tends to 1 as $s \to \infty$. Note that the equality holds independently of energy if $\sin^2\theta_{\mathrm{W}} = 0.25$, i.e. if $g_{\mathrm{V}}^{\mathrm{e}} = 0$.

Both neutral and charged currents contribute to reactions (II):

$$\nu_{\mathrm{e}}(k_1) + \mathrm{e}^-(p_1) \to \nu_{\mathrm{e}}(k_2) + \mathrm{e}^-(p_2) \qquad \text{(II.1)} ,$$

$$\overline{\nu}_{\mathrm{e}}(k_1) + \mathrm{e}^-(p_1) \to \overline{\nu}_{\mathrm{e}}(k_2) + \mathrm{e}^-(p_2) \qquad \text{(II.2)} .$$

For (II.1), the diagrams are Fig. 12.3b and Fig. 12.4, associated respectively with the Z^0 and W exchange in the t and u channels of the t and u variables defined in (33), i.e. their propagators are $(t - M_{\mathrm{Z}}^2)^{-1}$ and $(u - M_{\mathrm{W}}^2)^{-1}$ respectively. The amplitudes are referred to as $\mathcal{M}_{\mathrm{Z}}$ and $\mathcal{M}_{\mathrm{W}}$. Since both contribute to the reaction (II.1), their relative sign is important and turns out to be negative. To see how it arises, it may be convenient to go back to the second quantization of the fields that enter the composition of $\mathcal{M}_{\mathrm{Z}}$ and $\mathcal{M}_{\mathrm{W}}$. The latter are obtained from the products of the fermionic creation and destruction operators which yield the initial and final states when

applied to the vacuum state $|0\rangle$. Since these operators anticommute, their relative order is important. At g^2, they come from the time-ordered product $T[H(x)H(y)]$. To determine their relative sign, we consider the combinations

$$\text{for } \mathcal{M}_{\rm Z}: b_{\rm e}^\dagger(p_2)b_{\rm e}(p_1)b_\nu^\dagger(k_2)b_\nu(k_1) \text{ coming from } \overline{\psi}_{\rm e}(x)\psi_{\rm e}(x)\overline{\psi}_\nu(y)\psi_\nu(y) \ ,$$

$$\text{for } \mathcal{M}_{\rm W}: b_{\rm e}^\dagger(p_2)b_\nu(k_1)b_\nu^\dagger(k_2)b_{\rm e}(p_1) \text{ coming from } \overline{\psi}_{\rm e}(x)\psi_\nu(x)\overline{\psi}_\nu(y)\psi_{\rm e}(y) \ ,$$

where $b^\dagger$ (b) is the creation (destruction) fermionic operator (Chap. 3). In writing these amplitudes, we keep only in $T[H(x)H(y)]$ the order of the fermion fields. In $\mathcal{M}_{\rm Z}$, using the anticommutation relations of $b_j^\dagger, b_j$, we have

$$b_{\rm e}^\dagger b_{\rm e} b_\nu^\dagger b_\nu = +b_{\rm e}^\dagger b_\nu^\dagger b_\nu b_{\rm e} = -b_{\rm e}^\dagger b_\nu b_\nu^\dagger b_{\rm e} \ .$$

The extreme left (right) member of the above equation is related to $\mathcal{M}_{\rm Z}$ ($\mathcal{M}_{\rm W}$), so that the relative sign between $\mathcal{M}_{\rm Z}$ and $\mathcal{M}_{\rm W}$ is definitely -1. The expression of $\mathcal{M}_{\rm Z}(\nu_{\rm e} + {\rm e}^- \to \nu_{\rm e} + {\rm e}^-)$ is identical to that of $\mathcal{M}_{\rm Z}(\nu_\mu + {\rm e}^- \to \nu_\mu + {\rm e}^-)$ given above in (37). According to Feynman rules, the amplitude $\mathcal{M}_{\rm W}[\nu_{\rm e}(k_1) + {\rm e}^-(p_1) \to \nu_{\rm e}(k_2) + {\rm e}^-(p_2)]$ is

$$\begin{aligned}\mathcal{M}_{\rm W} &= \frac{G_{\rm F}}{\sqrt{2}} \frac{\overline{u}(k_2)\gamma^\mu(1-\gamma_5)u(p_1)\,\overline{u}(p_2)\gamma_\mu(1-\gamma_5)u(k_1)}{1-u/M_{\rm W}^2} \\ &= \frac{-G_{\rm F}}{\sqrt{2}} \frac{\overline{u}(k_2)\gamma^\mu(1-\gamma_5)u(k_1)\,\overline{u}(p_2)\gamma_\mu(1-\gamma_5)u(p_1)}{1-u/M_{\rm W}^2} \ , \end{aligned} \tag{12.47}$$

after a Fierz rearrangement (Appendix). For low neutrino energy, we may neglect $-t/M_{\rm Z}^2$ and $-u/M_{\rm W}^2$ in (37) and (47). The relative minus sign can be conventionally put into $\mathcal{M}_{\rm Z}$, so the total amplitude of the reaction (II.1) is $\mathcal{M} = \mathcal{M}_{\rm W} - \mathcal{M}_{\rm Z}$. Combining (37) and the second line of (47), we get

$$\begin{aligned}&\mathcal{M} = \frac{-G_{\rm F}}{\sqrt{2}}\overline{u}(k_2)\gamma^\mu(1-\gamma_5)u(k_1)\,\overline{u}(p_2)\gamma_\mu(g'_{\rm V} - g'_{\rm A}\gamma_5)u(p_1) \ , \\ &g'_{\rm V} = 1 + g_{\rm V}^{\rm e} = +\tfrac{1}{2} + 2\sin^2\theta_{\rm W} \ \ ; \ \ g'_{\rm A} = 1 + g_{\rm A}^{\rm e} = +\tfrac{1}{2} \ \ . \end{aligned} \tag{12.48}$$

The forward amplitude $\mathcal{M}(E_\nu, q^2 = 0)$ of (II.1) can be readily obtained from (48) by putting $k_1 = k_2$, $p_1 = p_2$ and we recover (19) after summing and averaging over the electron spin states. The cross-section is now readily obtained using (45) and (46) as examples. We have

$$\begin{aligned}\frac{{\rm d}\sigma(\nu_{\rm e} + {\rm e}^- \to \nu_{\rm e} + {\rm e}^-)}{{\rm d}y} &= \frac{G_{\rm F}^2 m E_\nu}{2\pi}\left[(g'_{\rm V} + g'_{\rm A})^2 + (g'_{\rm V} - g'_{\rm A})^2(1-y)^2\right] \\ &= \frac{G_{\rm F}^2 m E_\nu}{2\pi}\left[(g_{\rm V}^{\rm e} + g_{\rm A}^{\rm e} + 2)^2 + (g_{\rm V}^{\rm e} - g_{\rm A}^{\rm e})^2(1-y)^2\right] \ , \end{aligned}$$

$$\sigma(\nu_{\rm e} + {\rm e}^- \to \nu_{\rm e} + {\rm e}^-) = \frac{G_{\rm F}^2 m E_\nu}{2\pi}\left[(g_{\rm V}^{\rm e} + g_{\rm A}^{\rm e} + 2)^2 + \frac{1}{3}(g_{\rm V}^{\rm e} - g_{\rm A}^{\rm e})^2\right] \ . \tag{12.49}$$

The amplitude of the reaction (II.1) in (48) is to be compared with (37) of the reactions (I). The cross-section of (II.2) is deduced from (49) by the substitution $g'_{\rm A} \leftrightarrow -g'_{\rm A}$ or $1 \leftrightarrow (1-y)^2$:

$$\frac{{\rm d}\sigma(\overline{\nu}_{\rm e} + {\rm e}^- \to \overline{\nu}_{\rm e} + {\rm e}^-)}{{\rm d}y} = \frac{G_{\rm F}^2 m E_\nu}{2\pi}\left[(g_{\rm V}^{\rm e} - g_{\rm A}^{\rm e})^2 + (g_{\rm V}^{\rm e} + g_{\rm A}^{\rm e} + 2)^2(1-y)^2\right] ,$$

$$\sigma(\overline{\nu}_{\rm e} + {\rm e}^- \to \overline{\nu}_{\rm e} + {\rm e}^-) = \frac{G_{\rm F}^2 m E_\nu}{2\pi}\left[(g_{\rm V}^{\rm e} - g_{\rm A}^{\rm e})^2 + \frac{1}{3}(g_{\rm V}^{\rm e} + g_{\rm A}^{\rm e} + 2)^2\right] . \quad (12.50)$$

Finally, the scattering amplitude of the pure charged currents reaction (III), $\nu_\mu(k_1) + {\rm e}^-(p_1) \to \mu^-(p_2) + \nu_{\rm e}(k_2)$ is similar to the $\mu^- \to {\rm e}^- + \nu_\mu + \overline{\nu}_{\rm e}$ decay. It is given by

$$\mathcal{M}(\nu_\mu + {\rm e}^- \to \mu^- + \nu_{\rm e}) = \frac{G_{\rm F}}{\sqrt{2}}\overline{u}(p_2)\gamma^\mu(1-\gamma_5)u(k_1)\;\overline{u}(k_2)\gamma_\mu(1-\gamma_5)u(p_1) .$$

Using (45) with $g_{\rm V}^{\rm e} = g_{\rm A}^{\rm e} = 1$, the corresponding cross-section is

$$\sigma(\nu_\mu + {\rm e}^- \to \nu_{\rm e} + \mu^-) = \frac{2G_{\rm F}^2 m E_\nu}{\pi}\left[1 - \frac{m_\mu^2}{2mE_\nu}\right]^2 . \quad (12.51)$$

The last factor $(1 - m_\mu^2/2mE_\nu)^2$ is purely kinematic. Comparing the above equation with (45), the ratio of NC over CC cross-sections is

$$R_{\rm NC/CC} \equiv \frac{\sigma(\nu_\mu + {\rm e}^- \to \nu_\mu + {\rm e}^-)}{\sigma(\nu_\mu + {\rm e}^- \to \nu_{\rm e} + \mu^-)} = \frac{\frac{1}{4} - \sin^2\theta_{\rm W} + \frac{4}{3}\sin^4\theta_{\rm W}}{[1 - (m_\mu^2/2mE_\nu)]^2} .$$

The integrated cross-sections of the reactions (I), (II) as given by (45), (46), (49), (50) can be represented in the $(g_{\rm V}^{\rm e}, g_{\rm A}^{\rm e})$ plane by four ellipses. Their intersections give two solutions for $g_{\rm V}^{\rm e}, g_{\rm A}^{\rm e}$ since the equations are symmetric by $(g_{\rm V}^{\rm e}, g_{\rm A}^{\rm e}) \longleftrightarrow -(g_{\rm V}^{\rm e}, g_{\rm A}^{\rm e})$. Precise measurements of the purely leptonic cross-sections come from the CHARM II collaboration at CERN, which gives $\sin^2\theta_{\rm W} = 0.2324 \pm 0.012$.

With this value of $\sin^2\theta_{\rm W}$, the gauge boson masses ${\rm W}^\pm$ and ${\rm Z}^0$ could be estimated long before their discoveries. Using formulas in Chap. 9, we get

$$M_{\rm W}^2 = \frac{\pi\alpha_{\rm em}}{\sqrt{2}G_{\rm F}\sin^2\theta_{\rm W}} \;\longrightarrow M_{\rm W} \approx 77.34\ {\rm GeV}\ \ ,\ \ M_{\rm Z} \approx 88.12\ {\rm GeV} .$$

Electroweak corrections at one-loop level will increase these tree-level masses by about 0.038%. The corrected masses agree very well with the experimental data, $M_{\rm W} = 80.33 \pm 0.15$ GeV, and $M_{\rm Z} = 91.187 \pm 0.007$ GeV.

From these studies of neutrino–electron scatterings, we draw another important conclusion: The *linear rise* of the cross-section with E_ν is characteristic of the neutrino scattered by a pointlike fermion. If the target has structure, its cross-section cannot increase at large E_ν.

12.5 Neutrino–Nucleon Elastic Scattering

As another example of the effects of the target structure, we consider the neutrino–nucleon scattering

$$\nu_\mu + \mathrm{N} \to \mu^- + \mathrm{N}' \quad , \quad \overline{\nu}_\mu + \mathrm{N} \to \mu^+ + \mathrm{N}' \; .$$

The study of these reactions enables us to familiarize ourself with the two important properties of the flavor-conserving V − A charged weak current $V_{\mathrm{ud}}\, \overline{u}\, \gamma_\mu (1-\gamma_5)\, d$, to wit, the conserved vector current (CVC) and the partial conservation of the axial current (PCAC) which are natural consequences of the standard electroweak model.

The amplitude $\nu_\mu(k_1) + \mathrm{n}(p_1) \to \mu^-(k_2) + \mathrm{p}(p_2)$ can be obtained from that of $\nu_\mu(k_1) + \mathrm{e}^-(p_1) \to \mu^-(k_2) + \nu_\mathrm{e}(p_2)$ by replacing the pointlike e–ν_e current $\overline{u}(p_2)\gamma_\mu(1-\gamma_5)u(p_1)$ by the nucleon n–p current:

$$\begin{aligned} V_{\mathrm{ud}} \, \langle \mathrm{p}(p_2) \,|\, V_\mu - A_\mu \,|\, \mathrm{n}(p_1) \rangle = & V_{\mathrm{ud}}\, \overline{u}(p_2) \Big\{ \gamma_\mu f_1(q^2) + \frac{\mathrm{i}\sigma_{\mu\nu} q^\nu}{2M} f_2(q^2) \\ & - g_1(q^2)\gamma_\mu\gamma_5 - g_3(q^2)\frac{q_\mu}{M}\gamma_5 \Big\}\, u(p_1) \; , \end{aligned} \tag{12.52}$$

where M is the nucleon mass and $q_\mu = (p_2 - p_1)_\mu$.

The nucleon form factors of V_μ are denoted by $f_{1,2}(q^2)$, those of the A_μ by $g_{1,3}(q^2)$. They are real by time-reversal invariance. From considerations of Lorentz covariance alone, the most general matrix element of $V_\mu - A_\mu$ has six form factors, three for V_μ and three for A_μ. Since form factors are induced by strong interactions which conserve G-parity (Chap. 6), only the terms even by G-parity transformations are kept. The four form factors in (52) satisfying this condition are said to be of the first class, following Weinberg. On the other hand, the two other terms odd under G-parity $f_3(q^2)$ and $g_2(q^2)$ respectively proportional to q_μ and $\mathrm{i}\sigma_{\mu\nu}q^\nu\gamma_5$ (second class current), are discarded. In any case, the q_μ term does not contribute if the current V_μ is conserved, i.e. if $q^\mu V_\mu = 0$ [see also (10.12)].

According to the CVC hypothesis postulated by Feynman and Gell-Mann, the vector part V_μ of the weak charged current, its Hermitian conjugate $V_\mu^\dagger$, and the isospin $I = 1$ component of the electromagnetic current, form an isotriplet. Now CVC is a direct consequence of the isospin structure of the weak charged current $\overline{u}\gamma_\mu d$ in the standard model. Indeed with the doublet q for the u, d quark fields, the three currents: $V_\mu = \overline{q}\gamma_\mu\tau^+\, q = \overline{u}\gamma_\mu d$, $V_\mu^\dagger = \overline{q}\gamma_\mu\tau^-\, q = \overline{d}\gamma_\mu u$, and $J_\mu^{\mathrm{em}}(I=1) = \frac{1}{2}\overline{q}\gamma_\mu\tau^3\, q = \frac{1}{2}(\overline{u}\gamma_\mu u - \overline{d}\gamma_\mu d)$ are the three components of an isovector (Chap. 9). CVC implies that the weak form factors $f_{1,2}(q^2)$ are equal to the electromagnetic form factors $F_{1,2}^1(q^2)$ which are given by (10.13) and (10.40) from electron–nucleon elastic scattering.

The contribution of $g_3(q^2)$ is proportional to the muon mass and can be neglected. We take $m_\mu = 0$ in the following. The contributions of

$f_1(q^2)$, $g_1(q^2)$ to the differential cross-section can be obtained from (41) with the replacement $g_{\rm V}^{\rm e} \longrightarrow f_1$, $g_{\rm A}^{\rm e} \longrightarrow g_1$. We only have to compute the contributions of $f_2(q^2)$ and get ($Q^2 = -q^2 > 0$)

$$\frac{{\rm d}\sigma}{{\rm d}Q^2} = \frac{G_{\rm F}^2 |V_{\rm ud}|^2}{4\pi} \left[(f_1+g_1)^2 + (f_1-g_1)^2 \left(1 - \frac{Q^2}{2ME_\nu}\right)^2 + (g_1^2 - f_1^2)\frac{Q^2}{2E_\nu^2} \right.$$
$$\left. + f_2^2 \frac{Q^2}{2M^2}\left(1 - \frac{Q^2}{2ME_\nu} + \frac{Q^2}{4E_\nu^2}\right) + f_1 f_2 \frac{Q^4}{2M^2E_\nu^2} + g_1 f_2 \left(\frac{2Q^2}{ME_\nu} - \frac{Q^4}{2M^2E_\nu^2}\right)\right] .$$

To obtain the antineutrino–nucleon cross-section $\sigma(\overline{\nu}_\mu + {\rm p} \to \mu^+ + {\rm n})$, we follow the discussions preceding (46) and simply replace $g_1(q^2)$ by $-g_1(q^2)$ in the above equation. The value of the differential cross-section at $q^2 = 0$ is *independent* of the incident neutrino energy and takes a simple form

$$\left.\frac{{\rm d}\sigma(\nu_\mu + {\rm n} \to \mu^- + {\rm p})}{{\rm d}Q^2}\right|_{q^2=0} = \frac{G_{\rm F}^2 |V_{\rm ud}|^2}{2\pi} \left[f_1^2(0) + g_1^2(0)\right] .$$

As stated, the form factors $f_{1,2}(q^2)$ are equal to $F_{1,2}^1(q^2)$ [cf. (10.40)]:

$$f_1(q^2) = F_1^1(q^2) \; ; \; f_2(q^2) = F_2^1(q^2) \; ; \text{hence } f_1(0) = 1 \; ; \; f_2(0) = 3.7 \; .$$

Therefore measurements of the neutrino–nucleon differential cross-section ${\rm d}\sigma/{\rm d}q^2$ enable us to determine the remaining $g_1(q^2)$, in particular $g_1(0)$. The value $g_1(0) \approx 1.25$ can also be determined from neutron β-decay in which the same flavor-conserving charged current is involved (Problem 13.6). Experiments show that the q^2 dependence of $g_1(q^2)$ is of the dipole type, $g_1(q^2) = 1.25 \times \left(1 - \frac{q^2}{M_A^2}\right)^{-2}$, with a pole mass $M_A \approx 0.95$ GeV.

PCAC and the Goldberger–Treiman Relation. The special case of zero momentum transfer $q^\mu = 0$ is illuminating. At $q^2 = 0$, the matrix element of the nucleon in (52) looks like the pointlike V − A quark current $V_{\rm ud}\, \overline{u}\gamma_\mu(1-\gamma_5)d$, the only change is in the form factor $g_1(0)$, which shifts to 1.25 from 1. Indeed, from (52) with $q^\mu = 0$, we have

$$V_{\rm ud} \, \langle {\rm p}(k) \,|\, V_\mu - A_\mu \,|\, {\rm n}(k) \rangle = V_{\rm ud}\, \overline{u}(k)\, \gamma_\mu \, [1 - g_1(0)\gamma_5] u(k) \; .$$

We know from CVC that $f_1(0)$ must be equal to 1, i.e. at $q^2 = 0$ the vector form factor $f_1(q^2)$ is not renormalized by the strong interaction. The pointlike vector coupling of quarks is exactly reflected on the hadronic level at $q^2 = 0$, because the hadronic vector current is conserved, i.e. $q^\mu V_\mu = 0$.

We would like to show that the value of $g_1(0) \approx 1.25$ has something to do with the partial conservation of the axial current (PCAC) which is a natural consequence of the small u, d quark mass m, $q^\mu A_\mu = 2m\, \overline{u}\gamma_5 d$. Let us examine the consequences of the massless quark ($m = 0$) or equivalently of

the conserved axial current. For that, we multiply the left- and the right-hand sides of (52) with q^μ. Thus,

$$q^\mu \,\langle \mathrm{p}(k_2)\,|\,A_\mu\,|\,\mathrm{n}(p_1)\rangle = \overline{u}(k_2)\,\left[2M\,g_1(q^2) + \frac{q^2}{M} g_3(q^2)\right]\gamma_5\,u(p_1)\;.$$

If the axial current is conserved, i.e. $q^\mu A_\mu = 0$, then

$$g_1(0) = \lim_{q^2\to 0}\;\frac{-q^2}{2M^2}\,g_3(q^2)\;. \tag{12.53}$$

Since $g_1(0) \neq 0$, the form factor $g_3(q^2)$ must have a pole at $q^2 = 0$ to cancel the numerator q^2. Such a pole implies the presence of a physical massless particle. There is one available, the nearly massless pion considered as a Goldstone–Nambu boson in the context of massless up and down quarks. The fact that the form factor $g_3(q^2)$ has a pion pole is clearly indicated in Fig. 12.9a, from which we derive

$$\overline{u}(k_2)\,g_3(q^2)\frac{q^\mu\gamma_5}{M}\,u(p_1)\,W_\mu = \left\{\sqrt{2}g_{\pi\mathrm{NN}}\overline{u}(k_2)\,\gamma_5\,u(p_1)\right\}\frac{\mathrm{i}}{q^2-m_\pi^2}\,[\mathrm{i}f_\pi q^\mu]\;W_\mu.$$

In the above equation, $\sqrt{2}\,g_{\pi\mathrm{NN}}$ is the charged pion–proton–neutron coupling constant in the effective pion–nucleon interaction $g_{\pi\mathrm{NN}}\overline{N}\,\gamma_5\,\tau^k\,N\phi_k$, where $\phi_k(x)$ is the pion field with the isospin index $k = 1, 2, 3$ [see (6.57–58)]. We then deduce

$$g_3(q^2) = \lim_{m_\pi^2\to 0}\frac{-\sqrt{2}f_\pi M g_{\pi\mathrm{NN}}}{q^2-m_\pi^2}\;.$$

Together with (53), one gets the Goldberger–Treiman (GT) relation which gives $g_1(0)$ in terms of $g_{\pi\mathrm{NN}}$ and the pion decay constant $f_\pi \approx 131$ MeV:

$$g_1(0) = \frac{f_\pi g_{\pi\mathrm{NN}}}{\sqrt{2}M}\;,\quad \text{GT relation}\;. \tag{12.54}$$

With $g_{\pi\mathrm{NN}}^2/(4\pi) \approx 13.5$, the GT relation is satisfied to 5% accuracy. PCAC is also written in a form which says that we may use $\partial^\mu A_\mu^k(x)$ to interpolate the pion field $\phi^k(x)$:

$$\partial^\mu A_\mu^k(x) = \frac{f_\pi m_\pi^2}{\sqrt{2}}\;\phi^k(x)\;,\quad \text{from}\;\left\langle 0\,\middle|\,A_\mu^k\,\middle|\,\pi^j(q)\right\rangle = \frac{\mathrm{i}f_\pi}{\sqrt{2}}\,q_\mu\delta^{kj}\;. \tag{12.55}$$

The above equation also tells us that the axial current is conserved in the limit $m_\pi \to 0$ of the Goldstone–Nambu massless pion.

We cannot leave PCAC without emphasizing that the conservation of the axial current with massless quarks is only valid at the tree level. Due

to quantum effects (illustrated by the triangle loop in Fig. 12.9b,c), even with massless quarks, for the isospin component $k = 3$ associated with π^0, the $\partial^\mu A^{k=3}_\mu$ no longer vanishes. In the presence of electromagnetic interactions, the conservation of both vector and axial currents is incompatible by loop corrections. To maintain gauge invariance (conservation of the vector current), we are led to $\partial^\mu A^3_\mu = (e^2/16\pi^2)\varepsilon^{\alpha\beta\rho\sigma}F_{\alpha\beta}F_{\rho\sigma}$ where $F_{\alpha\beta}$ is the electromagnetic field tensor defined in (2.132). This is called the Adler–Bell–Jackiw (ABJ) anomaly, which has a number of remarkable consequences, the most famous being the decay $\pi^0 \to 2\gamma$ for which the three colors of quarks exhibit their glaring evidence (see Further Reading).

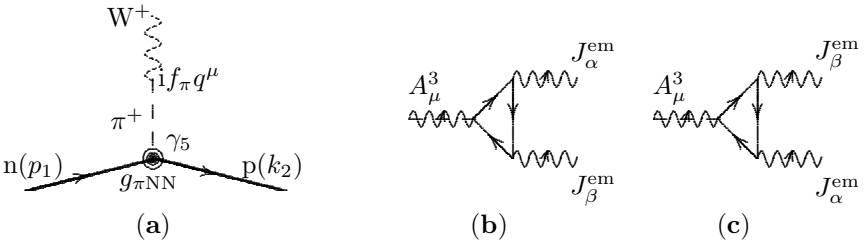

(**a**) (**b**) (**c**)

Fig. 12.9. (**a**) Pion pole dominance of the axial current ; (**b-c**) the ABJ anomaly of the Axial-Vector-Vector currents, related to the $\pi^0 \to 2\,\gamma$ decay

Another case of interest in the neutrino–nucleon cross-section is the high energy limit $2ME_\nu \gg Q^2$. The differential cross-section decreases quickly with Q^2 as the square of dipole form factors:

$$\frac{\mathrm{d}\sigma(\nu_\mu + \mathrm{n} \to \mu^- + \mathrm{p})}{\mathrm{d}Q^2} = \frac{G_\mathrm{F}^2|V_{\mathrm{ud}}|^2}{2\pi}\Big[f_1^2(q^2) + g_1^2(q^2) + \frac{Q^2}{4M^2}f_2^2(q^2)\Big]\,,$$

and the integrated cross-section σ is a constant $\sim G_\mathrm{F}^2\Lambda^2/3\pi$, where $\Lambda \approx 1$ GeV is the pole mass of the form factors. With pointlike targets, σ is linearly rising with E_ν; the contrast is striking. Numerically, this exclusive cross-section $\sigma(\nu_\mu + \mathrm{n} \to \mu^- + \mathrm{p}) \leq 10^{-38}$ cm^2 constitutes a tiny portion of the inclusive $\sigma(\nu_\mu + \mathrm{N} \to \mu^- + X)$ which we consider in the following section.

12.6 Neutrino–Nucleon Deep Inelastic Collision

One of the most dramatic evidences for quarks as fundamental constituents of hadrons is provided by data on deep inelastic neutrino–nucleon, its cross-section shows up as a *linearly rising* function of the incident neutrino energy. From experiments at CERN, FermiLab, and Serpukhov, with E_ν ranging over two orders of magnitude, from 2 to 260 GeV, the neutrino and antineutrino cross-sections continue to increase impressively (Fig. 12.10). This behavior is what we expect from neutrino scattering by a pointlike particle, illustrated by the previous study with the target electron. We remark that for $E_\nu \sim 300$ GeV, $s \sim 2ME_\nu \ll M_\mathrm{W}^2$, so that the linear approximation of the cross-section is still valid and the propagator effect of the W boson can be neglected.

12.6.1 Deep Inelastic Cross-Section

Deep inelastic neutrino–nucleon cross-section can be easily transcribed from that of deep inelastic electron–nucleon scattering; the photon exchange of the latter is replaced by the weak boson $\mathrm{W}^{\pm}$ or Z^0 of the former, depending on whether $\nu_\ell + \mathrm{N} \to \ell^- + X$ or $\nu_\ell + \mathrm{N} \to \nu_\ell + X$ process is observed. For definiteness, let us concentrate on charged current deep inelastic scattering (Fig. 12.11). The cross-section $\nu_\mu(p) + \mathrm{N}(P) \to \mu^-(p') + X$ can be obtained from $\mathrm{e}(p) + \mathrm{N}(P) \to \mathrm{e}(p') + X$ by (10.41) by the replacements

$$\text{couplings and propagators} \ : \ \frac{e^2}{q^2} \longrightarrow \Big(\frac{g}{2\sqrt{2}}\Big)^2 \frac{1}{q^2 - M_{\mathrm{W}}^2} \ = \frac{-G_{\mathrm{F}}}{\sqrt{2}(1 + \frac{Q^2}{M_{\mathrm{W}}^2})} \ ,$$

$$\text{lepton vertex} \ : \ \overline{\ell}\gamma^\mu \ell \longrightarrow \overline{\ell}\gamma^\mu(1-\gamma_5)\nu_\ell \ ,$$

$$\text{hadron vertex} \ : \ J_\mu^{\mathrm{em}} \equiv \overline{q}\gamma_\mu q \longrightarrow V_{\mathrm{Qq}}\,(V_\mu - A_\mu) \equiv V_{\mathrm{Qq}}\overline{Q}\gamma_\mu(1-\gamma_5)q \ . \quad (12.56)$$

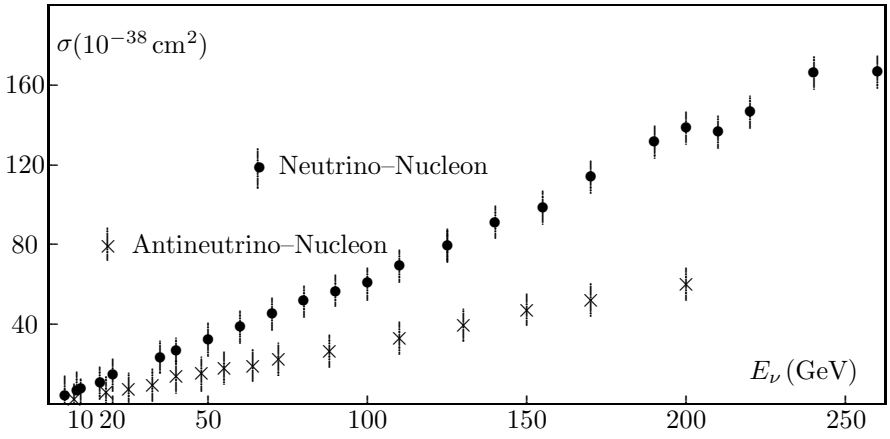

Fig. 12.10. $\sigma(\nu_\mu + \mathrm{N} \to \mu^- + X)$, $\sigma(\overline{\nu}_\mu + \mathrm{N} \to \mu^+ + X)$

Taking the square of the matrix element, the leptonic tensor $l^{\mu\nu}$ in (10.28) becomes now $\widetilde{l}^{\mu\nu}$. We have

$$\begin{aligned} \widetilde{l}^{\mu\nu}(p,p') &= 2\,\mathrm{Tr}[\not{p}'\gamma^\mu \not{p}\gamma^\nu(1-\gamma_5)] \\ &= 8\big(p^\mu p'^\nu + p^\nu p'^\mu - g^{\mu\nu} p\cdot p' - \mathrm{i}\,\varepsilon^{\mu\nu\alpha\beta}p_\alpha p'_\beta\big) \ . \end{aligned} \quad (12.57)$$

Compared with $l^{\mu\nu}$ in (10.28), we note the absence of the factor $(\frac{1}{2})$ of the spin average before the trace of $\widetilde{l}^{\mu\nu}$, since the incoming neutrino has only one helicity, contrary to the electron in $l^{\mu\nu}$. We have a factor of 2 because of $(1-\gamma_5)^2 = 2(1-\gamma_5)$ in $\widetilde{l}^{\mu\nu}$. For antineutrino $\overline{\nu}_\mu(p) + \mathrm{N}(P) \to \mu^+(p') + X$,

the modification in $\widetilde{l}^{\mu\nu}(p,p')$ is the interchange $p \leftrightarrow p'$. Hence we have $+\mathrm{i}\,\varepsilon^{\mu\nu\alpha\beta}p_\alpha p'_\beta$ in the corresponding $\widetilde{l}^{\mu\nu}$ of antineutrinos.

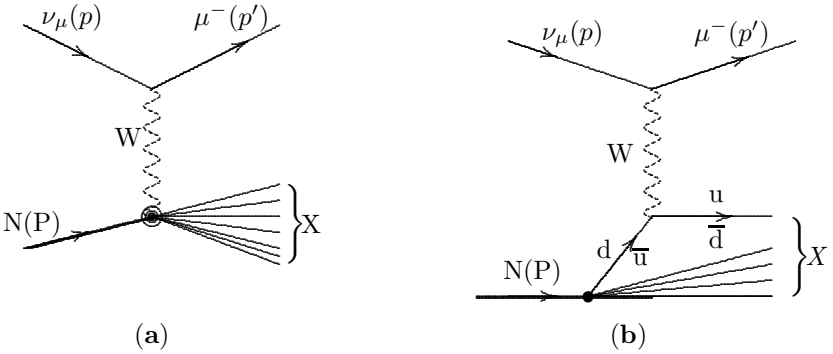

Fig. 12.11. (**a**) Deep inelastic neutrino–nucleon scattering by charged current; (**b**) $\nu_\mu + \mathrm{d}(\text{or } \overline{\mathrm{u}}) \to \mu^- + \mathrm{u}(\text{or } \overline{\mathrm{d}})$ at the parton level

As for the dimensionless hadronic tensor $\widetilde{W}_{\mu\nu}(P,q)$ – defined analogously to $W_{\mu\nu}(P,q)$ in (10.42) with the replacement (56) – it has both symmetric and antisymmetric parts due to the parity violating V×A of the weak currents. Contrary to electromagnetic currents which are conserved, weak currents are not: $q^\mu \widetilde{W}_{\mu\nu}(P,q) \neq 0$, therefore $\widetilde{W}_{\mu\nu}(P,q)$ has the maximum number of Lorentz-invariant terms. Following (10.43), we write

$$\widetilde{W}_{\mu\nu}(P,q) = 4\pi\Big\{-g_{\mu\nu}\widetilde{W}_1(q^2,\nu) + \frac{P_\mu P_\nu}{M^2}\widetilde{W}_2(q^2,\nu) - \frac{\mathrm{i}\,\varepsilon_{\mu\nu\alpha\beta}}{2M^2}P^\alpha q^\beta \widetilde{W}_3(q^2,\nu)$$
$$+ \frac{q_\mu q_\nu}{M^2}\widetilde{W}_4(q^2,\nu) + \frac{P_\mu q_\nu + P_\nu q_\mu}{2M^2}\widetilde{W}_5(q^2,\nu) + \frac{\mathrm{i}\,(P_\mu q_\nu - P_\nu q_\mu)}{2M^2}\widetilde{W}_6(q^2,\nu)\Big\}\,.$$

When $\widetilde{W}_{\mu\nu}(P,q)$ is multiplied by the leptonic tensor $\widetilde{l}^{\mu\nu}(p,p')$, the antisymmetric $(P_\mu q_\nu - P_\nu q_\mu)$ factor of $\widetilde{W}_6$ vanishes when contracted with $\varepsilon^{\mu\nu\alpha\beta}$ (because only three of the vectors p, p', q, P are independent). The other factors involved in $\widetilde{W}_{4,5}$ are proportional to the squared mass of the muon, and can be neglected. In the following, we take $m_\mu = 0$. Only three structure functions $\widetilde{W}_{1,2,3}(q^2,\nu)$ remain in the ν–N cross-section, instead of two $W_{1,2}(q^2,\nu)$ in the electron–nucleon deep inelastic cross-section. Using the general formula (10.41) together with the replacements (56), the neutrino deep inelastic cross-section $\mathrm{d}\sigma_{\mathrm{in}}$ is given by

$$\mathrm{d}\sigma_{\mathrm{in}}(\nu_\mu + \mathrm{N} \to \mu^- + X) = \frac{1}{2(s-M^2)}\frac{G_{\mathrm{F}}^2}{2}\frac{1}{(1+\frac{Q^2}{M_W^2})^2}\widetilde{l}^{\mu\nu}\widetilde{W}_{\mu\nu}\frac{\mathrm{d}^3p'}{(2\pi)^3\,2E_{p'}}\,.$$

In the laboratory system $P = (M, \mathbf{0})$, $p = (E = |\boldsymbol{p}|, \boldsymbol{p})$, $p' = (E' = |\boldsymbol{p}'|, \boldsymbol{p}')$, $q^2 = (p-p')^2 = -2EE'\sin^2\frac{\theta}{2}$, $\nu \equiv P\cdot q/M = (E - E')$, we find

$$\widetilde{l}^{\mu\nu}\widetilde{W}_{\mu\nu} = 64\pi EE'\left\{2\widetilde{W}_1\sin^2\frac{\theta}{2} + \widetilde{W}_2\cos^2\frac{\theta}{2} + \widetilde{W}_3\frac{E+E'}{M}\sin^2\frac{\theta}{2}\right\}\,.$$

For $Q^2 \ll M_{\rm W}^2$, we can neglect the W boson propagator effects and obtain

$$\frac{{\rm d}\sigma^{\nu,\overline{\nu}}}{{\rm d}Q^2{\rm d}\nu} = \frac{G_{\rm F}^2}{2\pi\, M}\frac{E'}{E}\left\{2\widetilde{W}_1(q^2,\nu)\sin^2\frac{\theta}{2} + \widetilde{W}_2(q^2,\nu)\cos^2\frac{\theta}{2} \right.$$
$$\left. \pm\widetilde{W}_3(q^2,\nu)\frac{E+E'}{M}\sin^2\frac{\theta}{2}\right\} \ . \tag{12.58}$$

From the $p \leftrightarrow p'$ interchange mentioned above, the $+(-)$ sign corresponds to $\nu_\mu(\overline{\nu}_\mu)$. Like the electron scattering in (10.65), the neutrino cross-section may be conveniently recast in terms of the Bjorken variable x and the energy loss variable $y = \nu/E$. With ${\rm d}Q^2{\rm d}\nu = 2ME\,\nu\,{\rm d}x\,{\rm d}y$, (58) becomes

$$\frac{{\rm d}\sigma^{\nu,\overline{\nu}}}{{\rm d}x{\rm d}y} = \frac{G_{\rm F}^2 ME}{\pi}\left\{\widetilde{W}_1(x,q^2)x\,y^2 + \frac{\nu}{M}\widetilde{W}_2(x,q^2)\,(1-y)\right.$$
$$\left. \pm\frac{\nu}{M}\widetilde{W}_3(x,q^2)\,x\,y\left(1-\frac{y}{2}\right)\right\} \ . \tag{12.59}$$

12.6.2 Quarks as Partons

We immediately see in (59) that, when q^2 becomes very large and the structure functions $\widetilde{W}(x,q^2)$ do not vanish, the deep inelastic ν–N cross-section rises linearly with the neutrino energy E, exactly as if the neutrino were hitting a pointlike object. This feature is dramatically confirmed by experiments (Fig. 12.10) and is similarly found in the e–N deep inelastic scattering studied in Chap. 10. Both electromagnetic and weak currents are probing the same pointlike spin-$\frac{1}{2}$ constituents of the nucleon. In analogy with e–N deep inelastic scattering, we identify the partons as quarks and antiquarks. The parton picture discussed in the electromagnetic case can be extended to deep inelastic neutrino scattering. Let us then write the charged current cross-section of ν_μ scattered by a pointlike spin-$\frac{1}{2}$ object [quark $\rm Q_j$ or antiquark $\overline{\rm Q}_k$ of mass $m_{j,k}$ and four-momentum $k^\mu_{j,k} = z_{j,k}P^\mu$]. Using (45) and (46), with $g_V = g_A = 1$, in addition to the appropriate CKM mixing, and similar to (10.51) with the trick $\int {\rm d}x\,\delta(z-x) = 1$, we have

$$\frac{{\rm d}\sigma(\nu_\mu + {\rm Q}_j \to \mu^- + {\rm q}_1)}{{\rm d}x{\rm d}y} = |V_{{\rm Q}_j{\rm q}_1}|^2\ \frac{2G_{\rm F}^2 m_j E}{\pi}\ \delta(z_j - x)\ ,$$
$$\frac{{\rm d}\sigma(\nu_\mu + \overline{\rm Q}_k \to \mu^- + \overline{\rm q}_2)}{{\rm d}x{\rm d}y} = |V_{{\rm Q}_k{\rm q}_2}|^2\ \frac{2G_{\rm F}^2 m_k E}{\pi}(1-y)^2\ \delta(z_k - x)\ . \tag{12.60}$$

We remark that if a quark is hit by a neutrino, there is no y dependence; but when an antiquark is probed, the dependence is $(1-y)^2$. Similarly, the antineutrino–antiquark cross-section is y independent, while the antineutrino–quark cross-section [see (46)] varies as $(1-y)^2$. These distributions correspond to the V − A charged currents of the standard model. In models beyond the

standard model with a V + A coupling for hypothetic new quarks, we simply interchange 1 with $(1-y)^2$ or $Q(x)$ with $\overline{Q}(x)$ in (60). Deep inelastic cross-section is then the sum of parton cross-sections, each contribution is weighted by the distribution $Q_j(z_j)\,,\ \overline{Q}_k(z_k)$ in the nucleon.

As in (10.50)–(10.52), the contributions of quarks and antiquarks to the cross-section can be obtained from (60) (remember $m_{j,k} = Mz_{j,k}$, where M is the nucleon mass):

$$\sum_j \int \mathrm{d}z_j \frac{2G_\mathrm{F}^2 m_j E}{\pi} Q_j(z_j)\delta(z_j - x) = \sum_j \frac{2G_\mathrm{F}^2 ME}{\pi} x Q_j(x)\ ,$$

$$\sum_k \int \mathrm{d}z_k \frac{2G_\mathrm{F}^2 m_k E}{\pi} \overline{Q}_k(z_k)\delta(z_k - x)(1-y)^2 = \sum_k \frac{2G_\mathrm{F}^2 ME}{\pi} x \overline{Q}_k(x)(1-y)^2\ .$$

We have

$$\frac{\mathrm{d}\sigma^\nu}{\mathrm{d}x\mathrm{d}y} = \frac{2G_\mathrm{F}^2 ME}{\pi} x \sum_{j,k} \left[|V_{\mathrm{Q_j q_1}}|^2 Q_j(x) + |V_{\mathrm{Q_k q_2}}|^2 \overline{Q}_k(x)(1-y)^2\right]\ ,$$

$$\frac{\mathrm{d}\sigma^{\overline{\nu}}}{\mathrm{d}x\mathrm{d}y} = \frac{2G_\mathrm{F}^2 ME}{\pi} x \sum_{j,k} \left[|V_{\mathrm{Q_k q_2}}|^2 \overline{Q}_k(x) + |V_{\mathrm{Q_j q_1}}|^2 Q_j(x)(1-y)^2\right]\ . \quad (12.61)$$

Let us rewrite (59) as a power series in $(1-y)$:

$$\begin{aligned}\frac{\mathrm{d}\sigma^{\nu,\overline{\nu}}}{\mathrm{d}x\mathrm{d}y} =& \frac{G_\mathrm{F}^2 ME}{\pi} \left\{ x\left[\widetilde{W}_1 \pm \frac{\nu}{2M}\widetilde{W}_3\right] + \left[\frac{\nu}{M}\widetilde{W}_2 - 2x\,\widetilde{W}_1\right](1-y) \right. \\ & \left. + x\left[\widetilde{W}_1 \mp \frac{\nu}{2M}\widetilde{W}_3\right](1-y)^2 \right\}\ . \end{aligned} \quad (12.62)$$

In the parton picture, (61) is identified with (62). By comparing the coefficients of $(1-y)^n$ for $n = 0, 1, 2$ in the expressions in (61) and (62), we get

$$\begin{aligned} &\widetilde{W}_1(x,q^2) \to \widetilde{F}_1(x)\ \ ;\ \ \frac{\nu}{M}\widetilde{W}_2(x,q^2) \to \widetilde{F}_2(x)\ \ ;\ \ \frac{\nu}{M}\widetilde{W}_3(x,q^2) \to \widetilde{F}_3(x)\ ; \\ &\widetilde{F}_1(x) = \sum_{j,k} \left[|V_{\mathrm{Q_j q_1}}|^2 Q_j(x) + |V_{\mathrm{Q_k q_2}}|^2 \overline{Q}_k(x)\right] \quad ; \quad \widetilde{F}_2(x) = 2x\widetilde{F}_1(x)\ ; \\ &\widetilde{F}_3(x) = 2\sum_{j,k} \left[|V_{\mathrm{Q_j q_1}}|^2 Q_j(x) - |V_{\mathrm{Q_k q_2}}|^2 \overline{Q}_k(x)\right]\ . \end{aligned} \quad (12.63)$$

The structure functions $\widetilde{F}_2(x)$ and $\widetilde{F}_3(x)$ can be separated by writing the sum and difference of (62) for neutrino and antineutrino:

$$\begin{aligned} \frac{\mathrm{d}\sigma^{\nu\mathrm{N}} + \mathrm{d}\sigma^{\overline{\nu}\mathrm{N}}}{\mathrm{d}x\mathrm{d}y} &= \frac{G_\mathrm{F}^2 ME}{\pi}\widetilde{F}_2(x)\left[1 + (1-y)^2\right]\ , \\ \frac{\mathrm{d}\sigma^{\nu\mathrm{N}} - \mathrm{d}\sigma^{\overline{\nu}\mathrm{N}}}{\mathrm{d}x\mathrm{d}y} &= \frac{G_\mathrm{F}^2 ME}{\pi} x\,\widetilde{F}_3(x)\left[1 - (1-y)^2\right]\ . \end{aligned} \quad (12.64)$$

In (64), N stands either for the proton or the neutron. Let us specify what $Q_j(x)$ and $\overline{Q}_k(x)$ are. At the parton level (Fig. 12.11b), below the charmed hadron threshold, we have for reactions involving neutrinos

$$\nu_\mu + \mathrm{d} \to \mu^- + \mathrm{u} \quad , \quad \nu_\mu + \mathrm{s} \to \mu^- + \mathrm{u} \; ,$$
$$\nu_\mu + \overline{\mathrm{u}} \to \mu^- + \overline{\mathrm{d}} \quad , \quad \nu_\mu + \overline{\mathrm{u}} \to \mu^- + \overline{\mathrm{s}}.$$

We then deduce (taking for simplicity $|V_{\mathrm{ud}}|^2 + |V_{\mathrm{us}}|^2 = 1$)

$$\widetilde{F}_2^{\nu,\mathrm{p}}(x) = 2x\Big[|V_{\mathrm{ud}}|^2 d(x) + |V_{\mathrm{us}}|^2 s(x) + \overline{u}(x)\Big] = 2x\widetilde{F}_1^{\nu,\mathrm{p}}(x) \; ,$$
$$\widetilde{F}_3^{\nu,\mathrm{p}}(x) = 2\Big[|V_{\mathrm{ud}}|^2 d(x) + |V_{\mathrm{us}}|^2 s(x) - \overline{u}(x)\Big] \; , \tag{12.65}$$

where $u(x), d(x)$, and $s(x)$ are the up, down, and strange quark distributions inside the proton.

For antineutrino reactions, the corresponding structure functions are obtained from the above equation with the replacements of $q_j(x)$ with $\overline{q}_j(x)$ in $\widetilde{F}_{1,2}$ and $q_j(x)$ with $-\overline{q}_j(x)$ in $\widetilde{F}_3$, i.e.

$$\widetilde{F}_2^{\overline{\nu},\mathrm{p}}(x) = 2x\Big[u(x) + |V_{\mathrm{ud}}|^2\overline{d}(x) + |V_{\mathrm{us}}|^2\overline{s}(x)\Big] = 2x\widetilde{F}_1^{\overline{\nu},\mathrm{p}}(x) \; ,$$
$$\widetilde{F}_3^{\overline{\nu},\mathrm{p}}(x) = 2\Big[u(x) - |V_{\mathrm{ud}}|^2\overline{d}(x) - |V_{\mathrm{us}}|^2\overline{s}(x)\Big] \; . \tag{12.66}$$

As already discussed in (10.58), the up quark distribution in the neutron is $d(x)$ and the down quark distribution in the neutron is $u(x)$, by isospin invariance. Then

$$\widetilde{F}_2^{\nu,\mathrm{n}}(x) = 2x\Big[|V_{\mathrm{ud}}|^2 u(x) + |V_{\mathrm{us}}|^2 s(x) + \overline{d}(x)\Big] \; ,$$
$$\widetilde{F}_3^{\nu,\mathrm{n}}(x) = 2\Big[|V_{\mathrm{ud}}|^2 u(x) + |V_{\mathrm{us}}|^2 s(x) - \overline{d}(x)\Big] \; . \tag{12.67}$$

The structure function of an isoscalar target (sum of proton and neutron) probed by the neutrino is obtained using (65) and (67) (in which we put $|V_{\mathrm{ud}}|^2 \approx .95 = 1$, $|V_{\mathrm{us}}|^2 \approx 0.048 = 0$ for simplicity):

$$\widetilde{F}_2^{I=0} \equiv [\widetilde{F}_2^{\nu,\mathrm{p}}(x) + \widetilde{F}_2^{\nu,\mathrm{n}}(x)] = 2x\Big[u(x) + d(x) + \overline{u}(x) + \overline{d}(x)\Big] \; . \tag{12.68}$$

Comparing the above equation with (10.64) which gives the electromagnetic structure function $F_2^{I=0}$ of the same isoscalar target (deuteron), we get

$$\frac{\widetilde{F}_2^{I=0}}{F_2^{I=0}} \leq \frac{18}{5} \; . \tag{12.69}$$

The equality holds if in (10.64) we neglect the contribution of sea quarks $s(x), \overline{s}(x)$ to the electromagnetic structure function $F_2^{I=0}(x)$, which amounts

to at most 13.5%. If quarks had integral (and not fractional) charges, this ratio would be ≤ 2.

The structure functions $\frac{18}{5}F_2^{I=0}(x)$ and $\widetilde{F}_2^{I=0}(x)$, which are the main quantities measured in deep inelastic scattering, are plotted in Fig. 12.12. The agreement of data with (69) is remarkable and provides another strong confirmation of the fractional charges of quarks. With the photon γ and weak-boson $\mathrm{W}^{\pm}$ probes, the electron and the neutrino see the same constituents of the nucleon, and the quark fractional charges can be revealed.

Finally, from (61), the ratio of the integrated cross-sections $\sigma^{\nu,\mathrm{N}}/\sigma^{\overline{\nu},\mathrm{N}}$ gives the antiquark (sea) content of the nucleon:

$$R = \frac{\sigma^{\nu,\mathrm{N}}}{\sigma^{\overline{\nu},\mathrm{N}}} = \frac{3+\alpha}{1+3\alpha}\ , \qquad \alpha \equiv \frac{\int_0^1 \mathrm{d}x\, x\overline{Q}(x)}{\int_0^1 \mathrm{d}x\, xQ(x)} < 1\ . \tag{12.70}$$

If the sea is absent, the ratio would be 3. From data plotted in Fig. 12.10, the ratio R turns out to be $\sim 0.67E_\nu/0.3E_\nu \sim 2.23$, which corresponds to $\alpha \sim 0.135$.

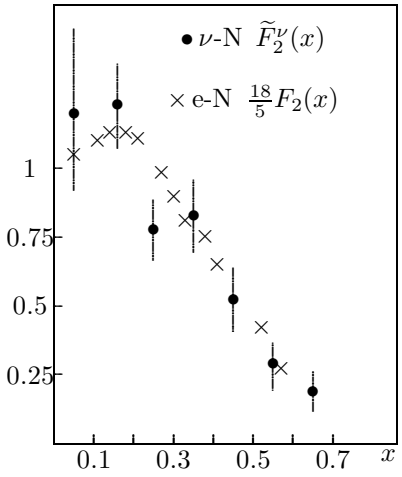

Fig. 12.12. Comparison of the isoscalar structure functions $\frac{18}{5}F_2(x)$ and $\widetilde{F}_2^{\nu}(x)$ as measured in electron and neutrino deep inelastic scatterings on nucleons. Data are taken from Fig. 8.12a of Perkins, D. H., *An Introduction to High Energy Physics* Addition-Wesley 1987. Adapted with permission of Addition-Wesley Longman Inc.

Problems

12.1 Leptons mixing. If the neutrinos are massive, the three doublets of leptons are mixed by $V_{\rm lep}$, analogously to the $V_{\rm CKM}$ of the quark sector. Then the leptonic flavors (or numbers) are no longer conserved, the decay $\mu^\pm \to {\rm e}^\pm + \gamma$ can occur. Draw the corresponding Feynman diagrams. Show qualitatively that the rate is proportional to $V_{\rm lep}$ and to the neutrino masses.

12.2 Solar neutrino flux. The solar heat flux received on earth is $\approx 1.95\,{\rm cal/cm^2/min}$, and the distance sun-earth is $\approx 1.5\times 10^8$ km. Deduce that the solar luminosity is $\approx 3.86\times 10^{33}$ erg /sec. According to the standard solar model, the sun shines by converting protons into helium (α):

$$4{\rm p} \to\ ({\rm He})^4_2 + 2{\rm e}^+ + 2\nu_{\rm e} + \gamma\ .$$

For every four protons consumed, this fusion produces about 26 MeV $= 4.16$ $\times 10^{-5}$ erg of thermal energy. How many fusions take place in the sun every second ? Show that there are $\approx 1.8\times 10^{38}$ neutrinos produced by the sun per second. Deduce that the solar neutrino flux at the surface of the earth is $\approx 6.4\times 10^{10}/{\rm cm^2/sec}$.

12.3 Effective neutrino mass in matter. Compute the effective mass of a neutrino of energy 10 MeV traveling in a supernova core (density $10^{14}\,{\rm g/cm^3}$) and in the solar core (density $100\,{\rm g/cm^3}$). Estimate the mean free path l of the neutrino.

12.4 Electromagnetic and weak decays of the π^0. Compute the weak decay rate $\pi^0 \to {\rm Z}^0 \to {\rm e}^+{\rm e}^-$, using $\pi^+ \to {\rm W}^+ \to {\rm e}^+\nu_{\rm e}$ as a guide. The electromagnetic decay width $\Gamma_{\rm em}(\pi^0 \to \gamma+\gamma \to {\rm e}^+ + {\rm e}^-)$ can be estimated to be $\sim (2\frac{\alpha m_{\rm e}}{M_\pi}\log\frac{m_{\rm e}}{M_\pi})^2\Gamma(\pi^0\to\gamma+\gamma)$. Draw the Feynman diagram of this cascade decay, and explain the origin of the coefficient $(\alpha m_{\rm e}/M_\pi)^2$. The logarithm term comes from a loop integral. From experimental data, the width $\Gamma(\pi^0\to\gamma+\gamma)$ is $2.5\times 10^{+12}$ larger than $\Gamma_W(\pi^+\to{\rm e}^+ + \nu_{\rm e})$; deduce that $\Gamma_W(\pi^0\to{\rm e}^+{\rm e}^-) \ll \Gamma_{\rm em}(\pi^0\to{\rm e}^+ + {\rm e}^-)$.

12.5 Neutrino sum rule. Just as for (10.62), show that

$$\int_0^1 {\rm d}x \widetilde{F}_3^{\nu,{\rm N}}(x) \equiv\ \tfrac{1}{2}\int_0^1 {\rm d}x\ \left[\widetilde{F}_3^{\nu,{\rm p}}(x) + \widetilde{F}_3^{\nu,{\rm n}}(x)\right] = 3\ ,$$

which tells us that the number of valence quarks in the nucleon is three. Again this sum rule agrees remarkably well with experiments.

12.6 Neutral current deep inelastic scattering. Write the differential cross-sections in terms of the parton distributions $u(x), d(x)$,etc. ,

$$\frac{{\rm d}\sigma}{{\rm d}x{\rm d}y}(\nu + {\rm N} \to \nu + X) \quad \text{and} \quad \frac{{\rm d}\sigma}{{\rm d}x{\rm d}y}(\overline{\nu} + {\rm N} \to \overline{\nu} + X)\ .$$

Derive the Paschos–Wolfenstein relation

$$\frac{\mathrm{d}\sigma^{\nu}_{\mathrm{NC}} - \mathrm{d}\sigma^{\overline{\nu}}_{\mathrm{NC}}}{\mathrm{d}\sigma^{\nu}_{\mathrm{CC}} - \mathrm{d}\sigma^{\overline{\nu}}_{\mathrm{CC}}} = |u_{\mathrm{L}}|^2 + |d_{\mathrm{L}}|^2 - |u_{\mathrm{R}}|^2 - |d_{\mathrm{R}}|^2 = \frac{1}{2} - \sin^2\theta_{\mathrm{W}} \ ,$$

which may be used to determine the Weinberg angle.

Suggestions for Further Reading

Neutrino mass, oscillations, MSW mechanism, solar neutrino deficit:

Bahcall, J., Calaprice, F., McDonald, A. and Toksuka, Y., *Solar Neutrino Experiments: The Next Generation*. Physics Today, July 1996

Bilenky, S. M. and Petcov, S. T., Rev. Mod. Phys. **59** (1987) 671

Kim, C. W. and Pevsner, A., *Neutrinos in Physics and Astrophysics*. Harwood Academic Publishers, Chur 1993

Neutral currents:

Binétruy, P., Maiani, L., Pessard, H., Rozanov, A., Smirnov, A. and Veltman, M., in *Neutral Currents Twenty Years Later*, Proc. Int. Conf. Paris 1993. (ed. Nguyen-Khac, Ung and Lutz, A. M.). World Scientific, Singapore 1994

Neutrino helicity (Goldhaber experiment); deep inelastic ν–N *scattering:*

Commins, E. D. and Bucksbaum, P. H., *Weak Interactions of Leptons and Quarks*. Cambridge U. Press, Cambridge 1983

Perkins, D. H., *Introduction to High Energy Physics* (Third edition). Addison-Wesley, Menlo Park, CA 1987

Anomalies:

Adler, S. L., in *Lectures on Elementary Particles Physics and Quantum Field Theory*, Proc. 1970 Brandeis Summer Institute (ed. Deser, S., Grisaru, M. and Pendleton, H.). MIT-Press, Cambridge 1970

Jackiw, R., in *Current Algebra and Anomalies* (ed. Treiman, S., Jackiw, R., Zumino, B. and Witten, E.). World Scientific, Singapore 1985

CVC, PCAC, *etc.* :

Scheck, F., *Electroweak and Strong Interactions*. Springer, Berlin, Heidelberg 1996